

Anelasticity and Attenuation:

D&T ch. 6

Hooke's law specifies that the stress \mathbb{T} at x, t depends only upon the instantaneous ϵ s at the same point x and time t . In an isotropic material:

$$\mathbb{T} = \kappa(\nabla \cdot \mathbf{s}) \mathbb{I} + 2\mu \delta$$

how to generalize to anisotropic — what are the complementary $\sigma(t)$ and $\epsilon(t)$

To account for damping we generalize this, retaining the linearity & spatial locality:

$$\mathbb{T}(x, t) = \int_{-\infty}^t \kappa(t-t') \nabla \cdot \frac{\partial \mathbf{s}}{\partial t'}(x, t') \mathbb{I} dt' + \int_{-\infty}^t 2\mu(t-t') \frac{\partial \delta}{\partial t'}(x, t') dt'$$

\mathbb{T} at time t now depends on entire previous strain history — Boltzmann superposition principle.

For simplicity let's denote strain by scalar $\epsilon(t)$ and complementary stress by $\sigma(t)$:

modulus $M(t)$	$\epsilon(t)$	$\sigma(t)$	remark
$\kappa(t)$	$\text{tr} \epsilon = \nabla \cdot \mathbf{s}$	$\frac{1}{3} \text{tr} \mathbb{T} = -dp$	isotropic deviatoric
$\mu(t)$	δ	$\mathbb{T} - \frac{1}{3}(\text{tr} \mathbb{T}) \mathbb{I}$	

Then write

$$\sigma(t) = \int_{-\infty}^t M(t-t') \frac{\partial \epsilon}{\partial t'}(t') dt'$$

lower limit $-\infty$: entire past history

upper limit t : causality, no dependence on future

Can alternatively relate strain to stress by

$$\varepsilon(t) = \int_{-\infty}^t J(t-t') \partial_{t'} \sigma(t') dt'$$

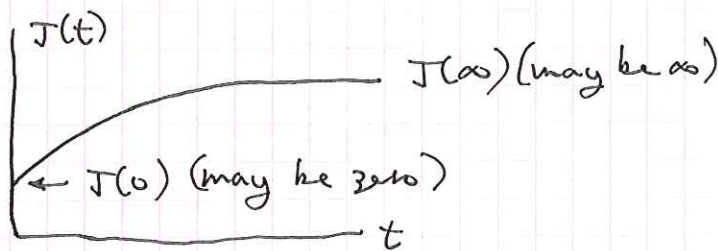
$M(t)$ called stress relaxation function.

$J(t)$ called creep function.

In a laboratory creep experiment — apply ~~stress~~
a unit step stress $\sigma(t) = H(t)$. Then

$$\varepsilon(t) = J(t)$$

$J(t)$ is the ~~strain~~
strain response to
a unit step stress

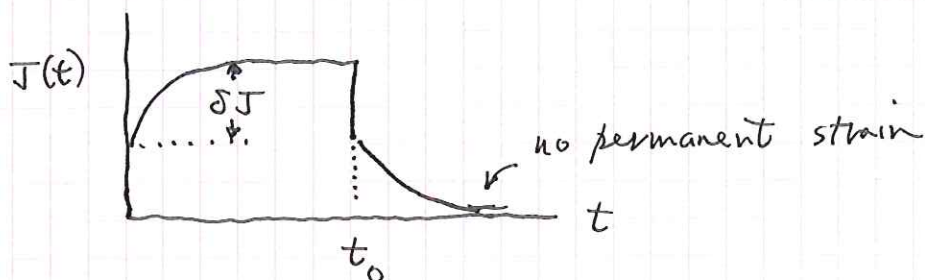
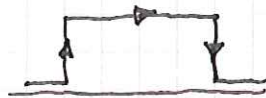


Define: $J_u = J(0)$ — unrelaxed or instantaneous elastic compliance

$J_r = J(\infty)$ — relaxed compliance ($= \infty$ in materials that exhibit steady-state creep)

An anelastic material has $J_u > 0$ and $J_r < \infty$ — such a material exhibits complete strain recovery in a creep cycle

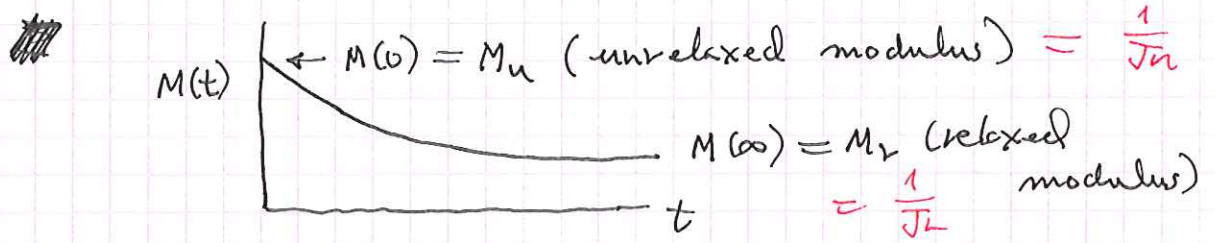
$$\sigma(t) = H(t) - H(t-t_0)$$



This a reasonable model on seismic time scales — no good for isostasy & post-glacial rebound.

The stress relaxation function is likewise the stress response to a unit step strain

$$\epsilon(t) = H(t) \iff \sigma(t) = M(t)$$

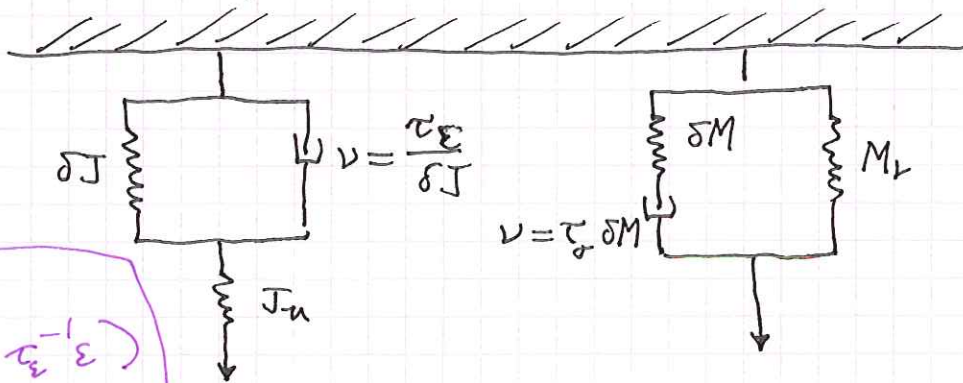


The stress required to maintain the unit strain relaxes with time — this the reason for the nomenclature. The difference $\delta M = M_u - M_r$ called the modulus defect.

end here lecture 11 with discussion of Maxwell & Kelvin Voigt

Standard linear solid:

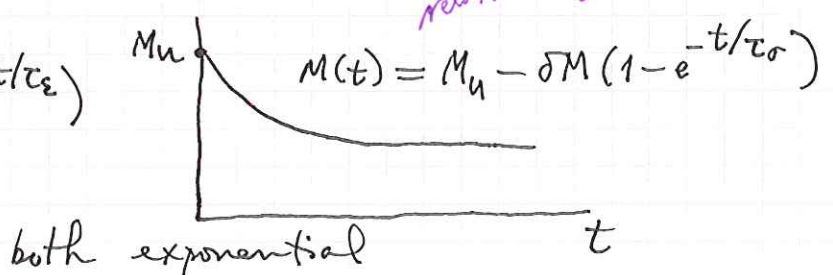
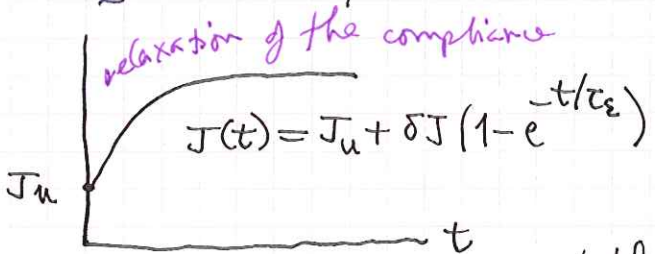
Simplest example of a material with both an instantaneous elastic response and complete creep recovery.



$$\dot{\epsilon} + \tau^{-1} \epsilon = M_u (\dot{\epsilon} + \tau_r^{-1} \epsilon)$$

The above two 3-parameter models are equivalent provided $\tau_r = \tau \delta M / \delta J$:

relaxation of the modulus or modulus defect



Harmonic variations:

systematically use ω for real freq and $\nu = \omega + i\alpha$ for complex

We have been considering static loading.

Suppose now that

$$\sigma(t) = \text{Re} [\sigma(\nu) e^{i\nu t}] \quad \text{where } \text{Im } \nu \leq 0$$

$$\varepsilon(t) = \text{Re} [\varepsilon(\nu) e^{i\nu t}]$$

How are the complex amplitudes $\sigma(\nu)$ and $\varepsilon(\nu)$ related?

$$\varepsilon(t) = \int_{-\infty}^t J(t-t') \partial_{t'} \sigma(t') dt'$$

$$\text{let } \xi = t - t'; \quad d\xi = -dt'; \quad \partial_{t'} = -\partial_{\xi}$$

$$= - \int_0^{\infty} J(\xi) \partial_{\xi} \sigma(t-\xi) d\xi$$

$$= - \int_0^{\infty} J(\xi) \partial_{\xi} \text{Re} [\sigma(\nu) e^{i\nu(t-\xi)}] d\xi$$

$$= \text{Re} [i\nu \int_0^{\infty} J(\xi) e^{-i\nu\xi} d\xi] \sigma(\nu) e^{i\nu t}$$

In summary: $\varepsilon(\nu) = J(\nu) \sigma(\nu)$ $M(\nu) J(\nu) = 1$
 $\sigma(\nu) = M(\nu) \varepsilon(\nu)$

$$J(\nu) = i\nu \int_0^{\infty} J(t) e^{-i\nu t} dt \quad \text{complex compliance}$$

$$M(\nu) = i\nu \int_0^{\infty} M(t) e^{-i\nu t} dt \quad \text{complex modulus}$$

Both are well-defined and analytic in the lower half-plane $\text{Im } \nu \leq 0$. Analytic continuation into upper half-plane will be singular. Note that $J(-\nu^*) = J^*(\nu)$ and $M(-\nu^*) = M^*(\nu)$ in lower halfplane

low and high-frequency limits:

$$\lim_{\nu \rightarrow 0} M(\nu) = \lim_{\nu \rightarrow 0} 1/J(\nu) = M_L = 1/J_L$$

relaxed at low freq.

$$\lim_{\nu \rightarrow \infty} M(\nu) = \lim_{\nu \rightarrow \infty} 1/J(\nu) = M_U = 1/J_U$$

unrelaxed at high freq.

On real frequency axis conventional to define real and imaginary parts by

$$M(\omega) = M_1(\omega) + iM_2(\omega)$$

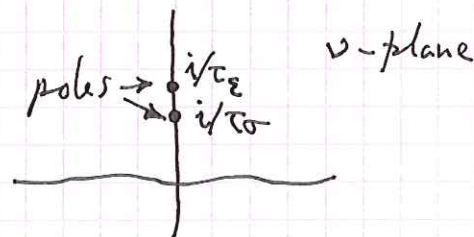
$$J(\omega) = J_1(\omega) - iJ_2(\omega)$$

Then $M_1(\omega)$ and $J_1(\omega)$ are even and $M_2(\omega)$ and $J_2(\omega)$ are odd functions of real ω .

The standard linear solid has:

$$M(\nu) = M_U - \delta M (1 + i\nu\tau_\sigma)^{-1}$$

$$J(\nu) = J_U + \delta J (1 + i\nu\tau_\epsilon)^{-1}$$



On the real axis:

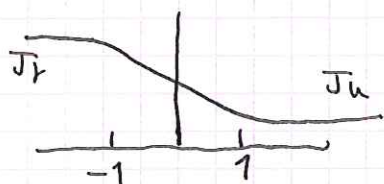
$$M_1(\omega) = M_U - \frac{\delta M}{1 + \omega^2 \tau_\sigma^2}$$

$$J_1(\omega) = J_U + \frac{\delta J}{1 + \omega^2 \tau_\epsilon^2}$$

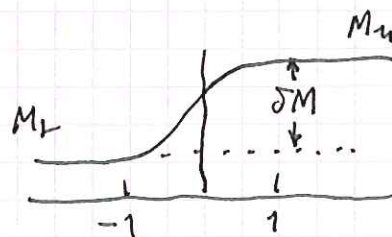
$$M_2(\omega) = \delta M \frac{\omega \tau_\sigma}{1 + \omega^2 \tau_\sigma^2}$$

$$J_2(\omega) = \delta J \frac{\omega \tau_\epsilon}{1 + \omega^2 \tau_\epsilon^2}$$

~~Plotted~~ Plotted versus $\log \omega$:



normal dispersion



called Debye relaxation peaks



x-axis labels wrong in DF-T FIG. 6.5

$\log \omega \tau_\sigma$

Energy dissipation and $Q(\omega)$:

The energy dissipated against internal friction per unit volume ~~in~~ in a ~~full~~ full cycle of (forced) oscillation at real frequency ω is

$$\oint \partial_t E dt = \oint \sigma \partial_t \varepsilon dt$$

$$\varepsilon(t) = \text{Re} [\varepsilon(\omega) e^{i\omega t}]$$

$$\sigma(t) = \text{Re} [\sigma(\omega) e^{i\omega t}]$$

$$\sigma(\omega) = M(\omega) \varepsilon(\omega)$$

write $\varepsilon(\omega) = |\varepsilon(\omega)| e^{i\Phi(\omega)}$

$$M(\omega) = |M(\omega)| e^{i\phi(\omega)}$$

then $\partial_t \varepsilon = -\omega |\varepsilon| \sin(\omega t + \Phi)$

$$\sigma = |M| |\varepsilon| \cos(\omega t + \Phi + \phi)$$

$$\oint \sigma \partial_t \varepsilon dt = -\omega |M| |\varepsilon|^2 \underbrace{\oint \cos(\omega t + \Phi + \phi) \sin(\omega t + \Phi) dt}_{*}$$

$$* = \oint \cos(\omega t + \Phi) \sin(\omega t + \Phi) dt \cos \phi$$

$$- \oint \sin^2(\omega t + \Phi) dt \sin \phi$$

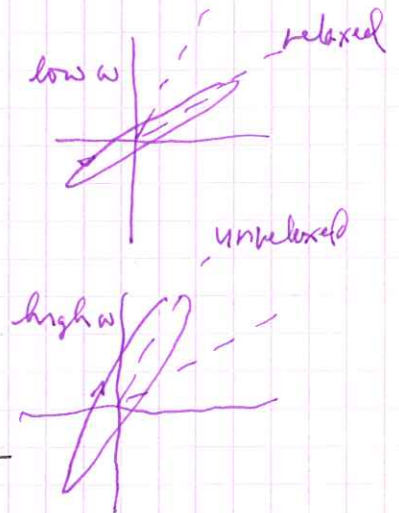
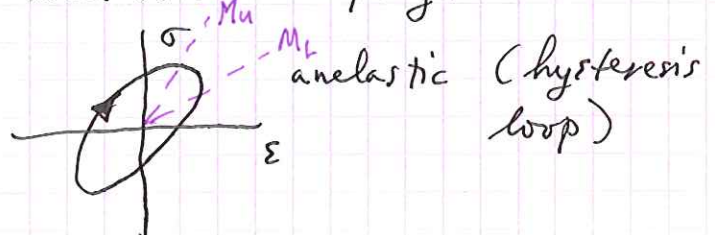
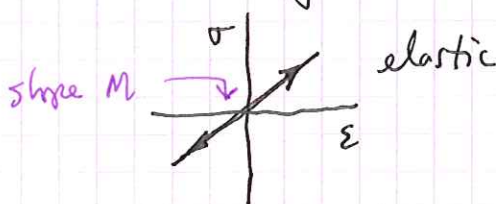
$$= -\frac{1}{2} \frac{2\pi}{\omega} \sin \phi = -\frac{\pi}{\omega} \sin \phi$$

average \nearrow \nwarrow length of cycle

$$\oint \sigma \partial_t \varepsilon dt = \pi |M| \sin \phi |\varepsilon|^2 = \pi M_2 |\varepsilon|^2$$

$$\oint \sigma \partial_t \varepsilon dt = \pi M_2(\omega) |\varepsilon(\omega)|^2 = \pi J_2(\omega) |\sigma(\omega)|^2$$

Imaginary part of modulus is thus a measure of the rate of anelastic damping:



The intrinsic quality factor is defined by

$$Q(\omega) = \frac{M_1(\omega)}{M_2(\omega)} = \frac{J_1(\omega)}{J_2(\omega)}$$

We also have $Q^{-1}(\omega) = \tan \phi(\omega)$ where $\phi(\omega)$ is the phase lag of the stress behind the strain in harmonic loading.

The average elastic energy stored in the springs can be shown to be (for a special class of materials that can be represented by a network of springs & dashpots)

$$\langle E \rangle = \frac{1}{4} M_1(\omega) |\varepsilon(\omega)|^2 = \frac{1}{4} |J_1(\omega)| |\varepsilon(\omega)|^2$$

In this case $Q(\omega)$ has an energetic interpretation:

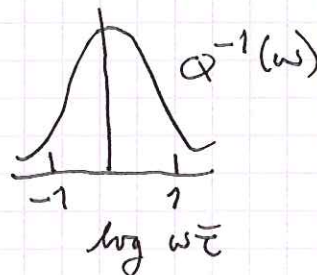
$$\frac{4\pi}{Q} = \frac{1}{\langle E \rangle} \int_{\text{cycle}} \dot{E} dt = \text{fractional energy dissipated - converted to heat - per cycle}$$

Example: standard linear solid

$$Q^{-1}(\omega) = \frac{\delta M}{\sqrt{M_1 M_2}} \left(\frac{\omega \bar{\tau}}{1 + \omega^2 \bar{\tau}^2} \right) \text{ where } \bar{\tau} = \sqrt{\tau_1 \tau_2}$$

Another Debye peak:

The dissipation in this case limited to a narrow frequency band.



Anelasticity in the Earth (and in geological materials in general) seems on the other hand to be characterized by constant (frequency-independent) $Q(\omega)$.

Relaxation spectrum:

$Q(\omega)$ in the earth is observed to be roughly independent of frequency within the band of interest in global seismology — from 0.3 mHz to 1 Hz. A useful model of such a material can be constructed by superposing standard linear solids with a continuous spectrum of relaxation times τ :

$$M(t) = M_u - \int_0^{\infty} \tau^{-1} \gamma(\tau) [1 - e^{-t/\tau}] d\tau$$

$$M(\nu) = M_u - \int_0^{\infty} \tau^{-1} \gamma(\tau) (1 + i\nu\tau)^{-1} d\tau$$

For real frequencies:

$$M_1(\omega) = M_u - \int_0^{\infty} \frac{\gamma(\tau)}{1 + \omega^2 \tau^2} \frac{d\tau}{\tau}$$

$$M_2(\omega) = \int_0^{\infty} \gamma(\tau) \frac{\omega\tau}{1 + \omega^2 \tau^2} \frac{d\tau}{\tau}$$

The weight factor $\gamma(\tau)$ is called the relaxation spectrum — it is a measure of the total contribution to the modulus defect from anelastic processes in the material with relaxation times between

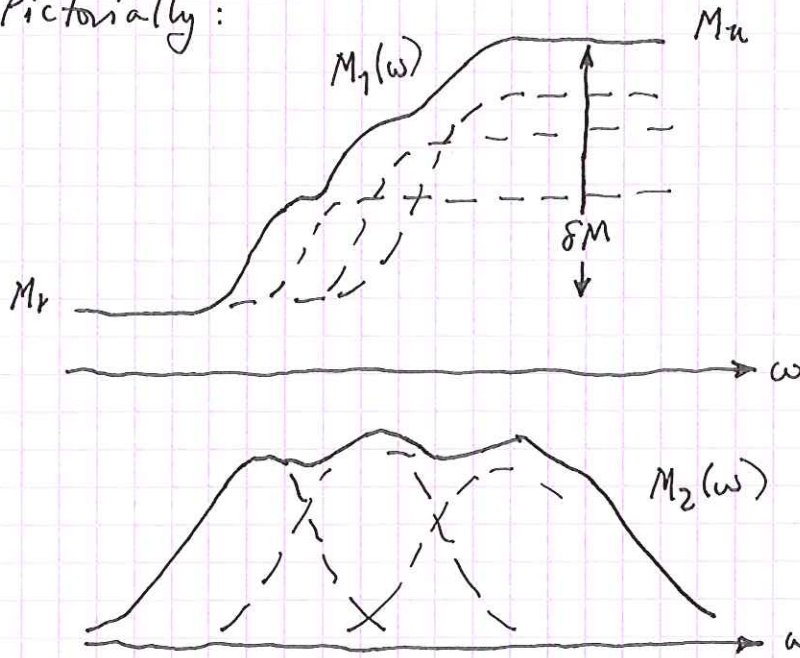
τ and $\tau + d\tau$:

$$\delta M = \int_0^{\infty} \tau^{-1} \gamma(\tau) d\tau$$

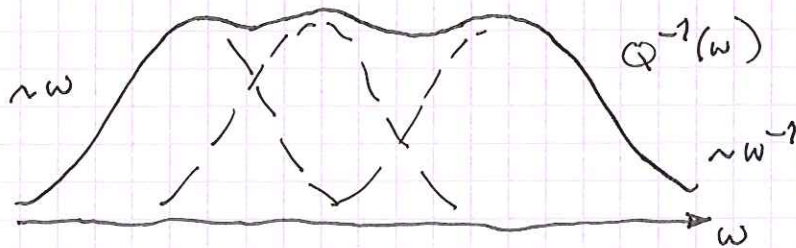
$$= \int_0^{\infty} \gamma(\tau) d(\ln \tau)$$

↙ this extra factor to force a logarithmic scaling is conventional

Pictorially:



The region where $M_2(\omega)$ is significant is called the absorption band — no significant attenuation above or below. $Q(\omega) = M_1(\omega)/M_2(\omega)$ looks \sim the same:



By adjusting the spectrum $\Upsilon(\tau)$ can attain any desired variation of $Q(\omega)$ within the absorption band.

Approximate relations:

Suppose now that $\Upsilon(\tau)$ is slowly varying over a broad range of relaxation times τ .

The Debye peak $\frac{\omega\tau}{1+\omega^2\tau^2}$ is peaked ~~at~~ at $\omega\tau=1$ and negligible outside $\frac{1}{10} \leq \omega\tau \leq 10$.

can write, approximately,

$$M_2(\omega) \approx \omega \Upsilon\left(\frac{1}{\omega}\right) \int_0^{\infty} \frac{d\tau}{1+\omega^2\tau^2}$$

$$= \Upsilon\left(\frac{1}{\omega}\right) \int_0^{\infty} \frac{dx}{1+x^2} = \frac{\pi}{2} \Upsilon\left(\frac{1}{\omega}\right)$$

The function $\frac{1}{1+\omega^2\tau^2}$ has a steplike character over the same range $\frac{1}{10} \leq \omega\tau \leq 10$.

see DFT
eq. (6.72)

Approximate by an abrupt step:

$$M_1(\omega) \approx M_u - \int_0^{1/\omega} \tau^{-1} \Upsilon(\tau) d\tau$$

Differentiate:

$$\frac{dM_1(\omega)}{d\omega} \approx \frac{1}{\omega} \Upsilon\left(\frac{1}{\omega}\right)$$

Comparing we obtain:

$$\frac{dM_1(\omega)}{d\omega} \approx \frac{2M_2(\omega)}{\pi\omega}, \quad \text{or}$$

$$\frac{d \ln M_1(\omega)}{d \ln \omega} \approx \frac{2}{\pi Q(\omega)}$$

Upon integrating:

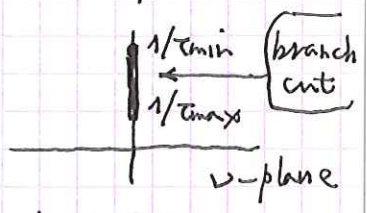
$$\frac{M_1(\omega)}{M_1(\omega_0)} \approx \exp \left[\frac{2}{\pi} \int_{\omega_0}^{\omega} \frac{d\omega'}{\omega' Q(\omega')} \right] \approx 1 + \frac{2}{\pi} \int_{\omega_0}^{\omega} \frac{d\omega'}{\omega' Q(\omega')}$$

where the last approximation assumes that $Q(\omega) \gg 1$.

Similar manipulations lead to a number of other approximations, e.g. $M_1(\omega) J_1(\omega) \approx 1$ and $M(t) J(t) \approx 1$.

Constant-Q absorption band model (Lin, Andersson & Kanamori 1976):

Consider the particular form of the spectrum

$$Y(\tau) = \begin{cases} \frac{\delta M}{\ln(\tau_{\max}/\tau_{\min})} & \text{if } \tau_{\min} \leq \tau \leq \tau_{\max} \\ 0 & \text{otherwise} \end{cases}$$


Evaluating the integral we find

$$M(\omega) = M_n - \frac{1}{2} \left[\frac{\delta M}{\ln(\tau_{\max}/\tau_{\min})} \right] \ln \left[\frac{i\nu + 1/\tau_{\min}}{i\nu + 1/\tau_{\max}} \right]$$

For real frequencies:

$$M_1(\omega) = M_n - \frac{1}{2} \left[\frac{\delta M}{\ln(\tau_{\max}/\tau_{\min})} \right] \ln \left[\frac{1 + \omega^2 \tau_{\min}^2}{\tau_{\min}^2/\tau_{\max}^2 + \omega^2 \tau_{\min}^2} \right]$$

$$M_2(\omega) = \left[\frac{\delta M}{\ln(\tau_{\max}/\tau_{\min})} \right] \arctan \left[\frac{\omega(\tau_{\max} - \tau_{\min})}{1 + \omega^2 \tau_{\min} \tau_{\max}} \right]$$

The quality factor $Q(\omega) = \frac{M_1(\omega)}{M_2(\omega)}$ is independent of frequency in the band $1/\tau_{\max} \ll \omega \ll 1/\tau_{\min}$.

It's value there is

$$Q^{-1} = \frac{\pi \delta M}{2 M_n \ln(\tau_{\max}/\tau_{\min})}$$

The real modulus within the same band is

$$M_1(\omega) \approx M_n \left[1 + \frac{2}{\pi Q} \ln(\omega \tau_{\min}) \right]$$

The ratio of the modulus at two frequencies is:

$$\frac{M_1(\omega)}{M_1(\omega_0)} \approx 1 + \frac{2}{\pi Q} \ln\left(\frac{\omega}{\omega_0}\right) \text{ — this can also be obtained from our earlier approximation.}$$

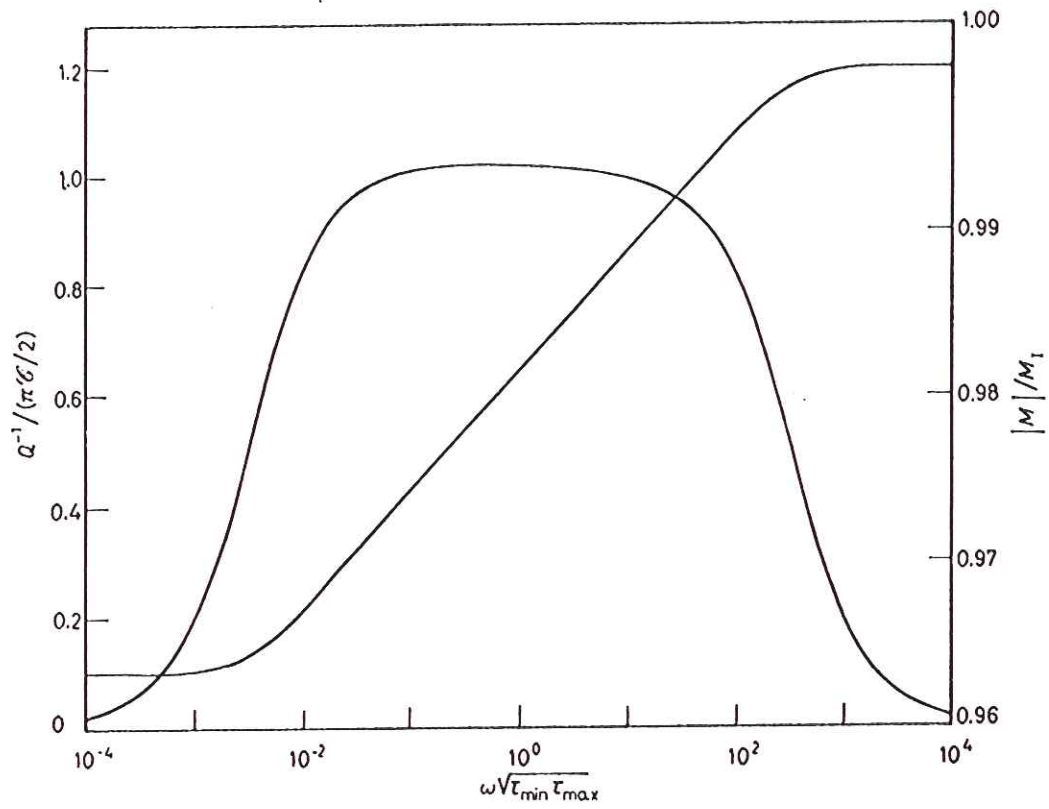


Fig. 3. - $Q^{-1}/(\pi\epsilon/2)$ and $|M|/M_1$ as functions of $\omega\sqrt{\tau_{\min}\tau_{\max}}$, $\tau_{\min}/\tau_{\max} = 10^{-5}$, $\epsilon = 100$.

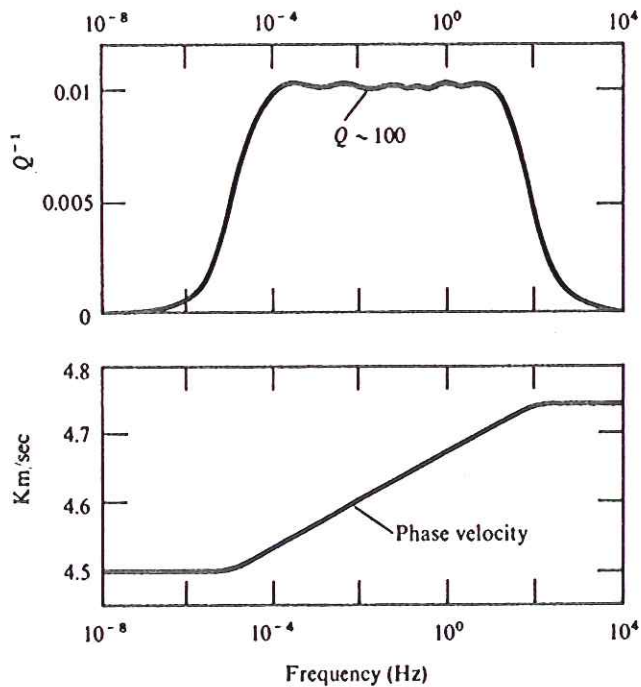


FIGURE 5.15
 Top. Internal friction values. Bottom. Phase velocities obtained (via (5.82)) from a superposition of 12 different relaxation peaks. [After Liu et al., 1976.]

Strictly constant-Q model (Kjartansson 1979)

No anelastic material has $Q(\omega)$ exactly constant for all $0 \leq \omega \leq \infty$. However, can find such a material if we relax the constraints $0 < M_2 \leq M_u < \infty$.

Consider the creep function

$$J(t) = \frac{(\omega_0 t)^\delta}{M_0 \Gamma(1+\delta)} H(t)$$

↑ gamma function

No instantaneous elastic response, creeps forever.

$$J(\nu) = i\nu \int_0^\infty J(t) e^{-i\nu t} dt \quad \text{is given by}$$

$$J(\nu) = \frac{1}{M_0} \left(\frac{i\nu}{\omega_0} \right)^{-\delta}$$

The complex modulus is the reciprocal of this:

$$M(\nu) = M_0 \left(\frac{i\nu}{\omega_0} \right)^\delta$$

On the real axis:

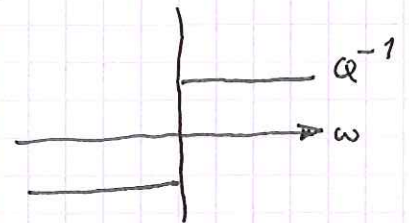
$$M_1(\omega) = M_0 \left| \frac{\omega}{\omega_0} \right|^\delta \sin\left(\frac{1}{2}\pi \operatorname{sgn} \omega\right)$$

$$M_2(\omega) = M_0 \left| \frac{\omega}{\omega_0} \right|^\delta \cos\left(\frac{1}{2}\pi \operatorname{sgn} \omega\right)$$

Thus

$$Q^{-1}(\omega) = \tan\left(\frac{1}{2}\pi\delta\right) \operatorname{sgn} \omega$$

$$\delta = \frac{1}{\pi} \arctan \frac{1}{Q} \approx \frac{1}{\pi Q}$$



The dispersion law is

$$\frac{M_1(\omega)}{M_1(\omega_0)} \approx \left(\frac{\omega}{\omega_0} \right)^\delta = \exp \left[\frac{2}{\pi} \arctan\left(\frac{1}{Q}\right) \ln\left(\frac{\omega}{\omega_0}\right) \right]$$

$$\approx 1 + \frac{2}{\pi Q} \ln\left(\frac{\omega}{\omega_0}\right)$$

same as
before

Logarithmic dispersion a very robust result — as long as $Q(\omega) \approx \text{constant}$ within some band (as observed in the Earth) — ~~insensitive~~ insensitive to behavior outside the band.

In summary, we can account for anelasticity within the Earth ~~in~~ in seismology by replacing the real elastic bulk & shear moduli by

$$\kappa(\omega) [1 + i Q_{\kappa}^{-1} \text{sgn } \omega]$$

$$\mu(\omega) [1 + i Q_{\mu}^{-1} \text{sgn } \omega]$$

↑ bulk and shear quality factors

$$\frac{\kappa(\omega)}{\kappa(\omega_0)} \approx 1 + \frac{2}{\pi Q_{\kappa}} \ln \left(\frac{\omega}{\omega_0} \right)$$

$$\frac{\mu(\omega)}{\mu(\omega_0)} \approx 1 + \frac{2}{\pi Q_{\mu}} \ln \left(\frac{\omega}{\omega_0} \right)$$

Shear attenuation is much more significant than bulk attenuation so that $Q_{\kappa} \gg Q_{\mu}$.

A slight amount of bulk dissipation is required somewhere within the Earth to account for the damping of the radial modes.

In a polycrystalline material, expect

$Q_{\kappa}/Q_{\mu} \approx 50-100$ due to local mismatch of elastic moduli at neighboring grains — macroscopic compressive deformation \Rightarrow microscopic shear

(~~Heinz~~ Heinz, Jeanloz, O'Connell 1982).

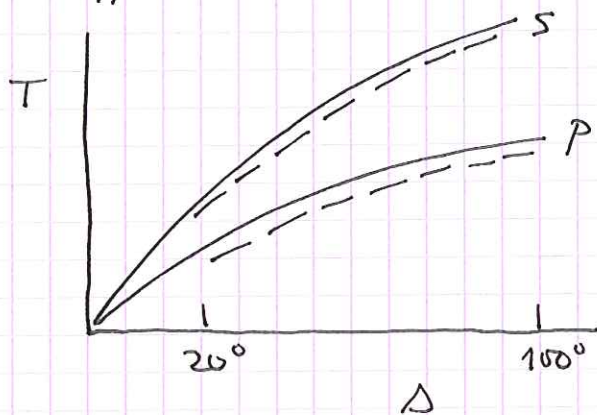
Average Q_{μ} in mantle is $Q_{\mu}^{-1} = \frac{1}{250} \pm 2\%$

Average in inner core $Q_{\mu}^{-1} = \frac{1}{110} \pm 25\%$

(Widmer, Masters & Gilbert 1991)

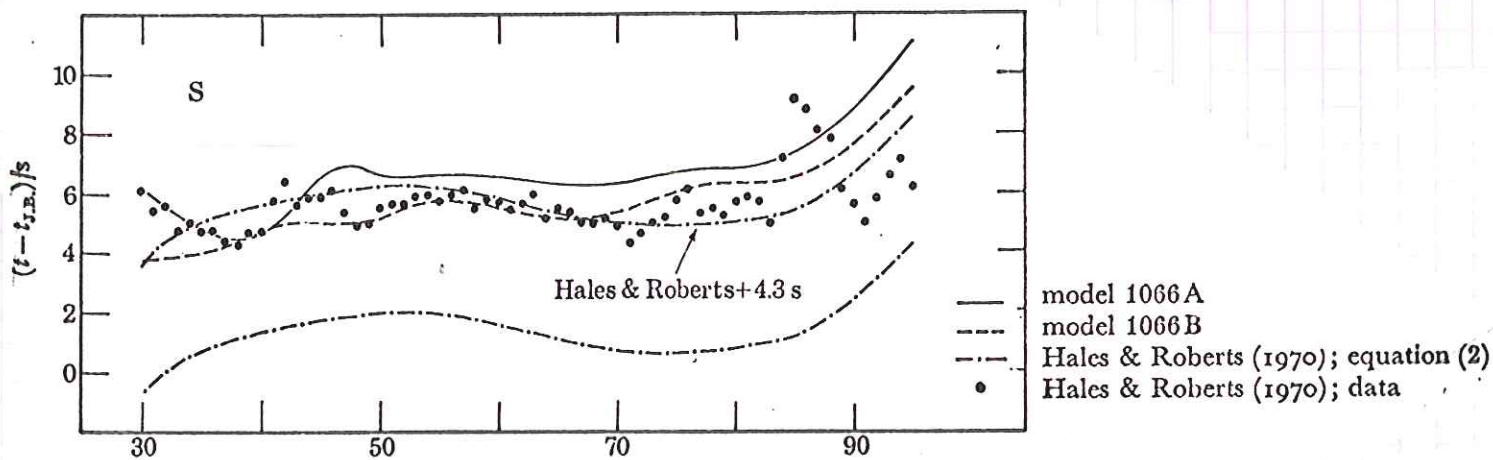
The associated dispersion provides a natural explanation of the travel-time baseline discrepancy.

Reliable SNREI models $p(r)$, $\kappa(r)$, $\mu(r)$ obtained by fitting normal mode eigenfrequencies first appeared in 1970's.



— theoretical $T-\Delta$
for a normal
mode Earth model
--- observed travel
times

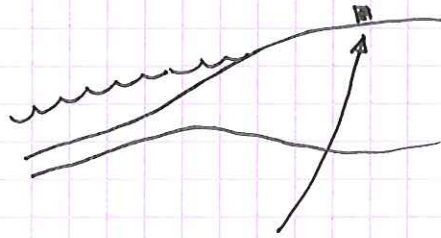
Observed P times 1-2 s early, observed
S times 4-5 s early from 20° to core shadow



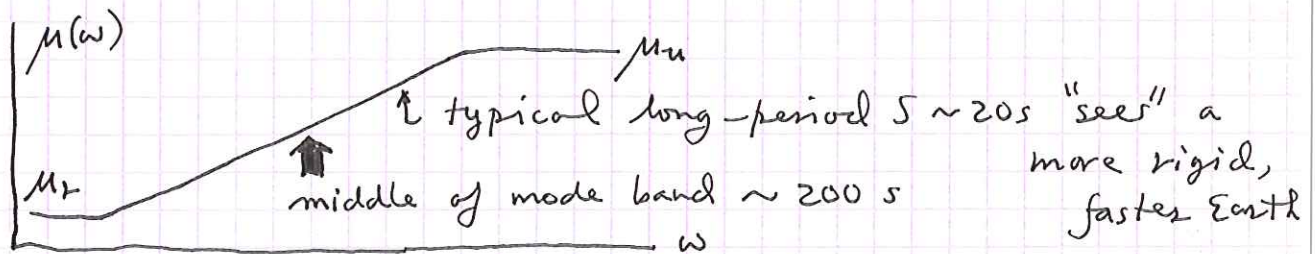
Note the confidence of the modellers (Dziewonski and Gilbert) — they have adjusted the data to get a fit!

Several rationalizations were suggested:

1. hard to measure absolute travel times because (quake location + measuring T) is a bootstrap operation.
2. continental bias — all seismic stations on land — modes see a global average



In 1976 Akopyan, Zharkov et al and Liu, Anderson and Kanamori "discovered" dispersion



$$\frac{\delta\mu}{\mu} \approx \frac{2}{250\pi} \ln\left(\frac{200s}{20s}\right) \approx 0.005 \quad \text{0.5\% more rigid at 20s than at 200s.}$$

$$S \text{ velocity } \beta = \sqrt{\mu/\rho} \quad \delta\beta/\beta = \frac{1}{2} \delta\mu/\mu = 0.25\% \text{ at 200s.}$$

Travel time of an S wave at $\Delta \sim 70^\circ$ is ~ 20 min.

The observed time should be faster by $\frac{2}{3}$ of $(\frac{1800s}{1200}) (0.0025) \sim \frac{4.5}{3}$ secs — the baseline discrepancy

The near constancy beyond $\Delta \sim 20^\circ$ is ~~due to the fact that the strongest attenuation is in the upper mantle.~~

If we make the (not very good) approximation that Q_K and Q_μ are constant within Φ :

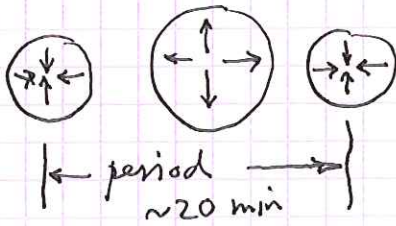
$\frac{1}{Q_K} \approx \frac{\nu_c}{Q_K} + \frac{\nu_s}{Q_\mu}$ where ν_c and ν_s are the fractional compressional and shear elastic energy of the mode

$$\nu_c = \frac{\int_{\Phi} \kappa (\nabla \cdot \mathbf{s})^2 dV}{\omega^2 \int_{\Phi} \rho \mathbf{s} \cdot \mathbf{s} dV}, \quad \nu_s = \frac{\int_{\Phi} 2\mu (\delta : \delta) dV}{\omega^2 \int_{\Phi} \rho \mathbf{s} \cdot \mathbf{s} dV}$$

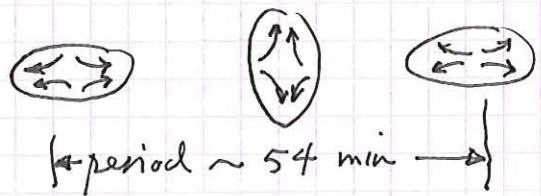
$\nu_c + \nu_s = 1$ (or $\nu_c + \nu_s + \nu_g = 1$ when we include the effect of gravity)

A simple example:

$0S_0$ (fundamental radial mode)



$0S_2$ (fundamental spheroidal mode — "football" mode)



mode	ν_c	ν_s	ν_g	Q
$0S_0$	1.304	0.028	-0.332 (destabilizing)	~ 6000
$0S_2$	0.115	0.546	0.339	~ 300

$0S_0$ has very little shear deformation — almost entirely compressional.

The Q of $0S_2$ is not well determined but is about 300. One expects the Q of $0S_0$ to be much higher if $Q_K \gg Q_\mu$.

Roughly:

$$Q(\sigma_0) \approx 300 \left(\frac{0.546}{0.028} \right) \sim 6000$$

↑
 $Q(\sigma_2)$

Riedesel et al. (1979) find $Q(\sigma_0) \sim 6000$ from a 2000 hour ~~stack~~ (!) stack of IDA records after the Indonesian earthquake.

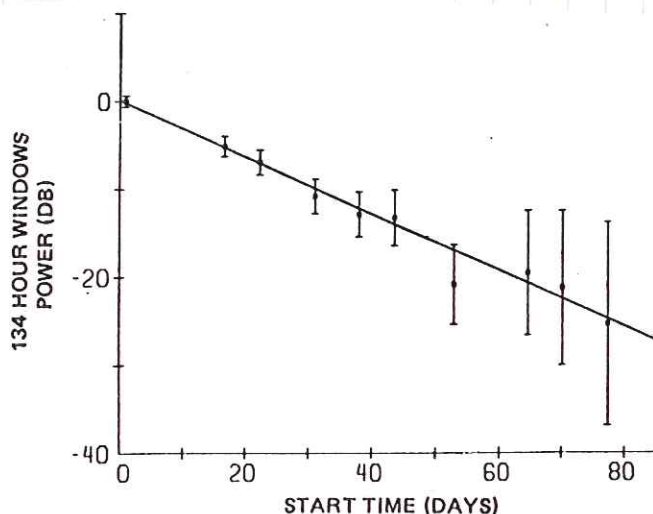
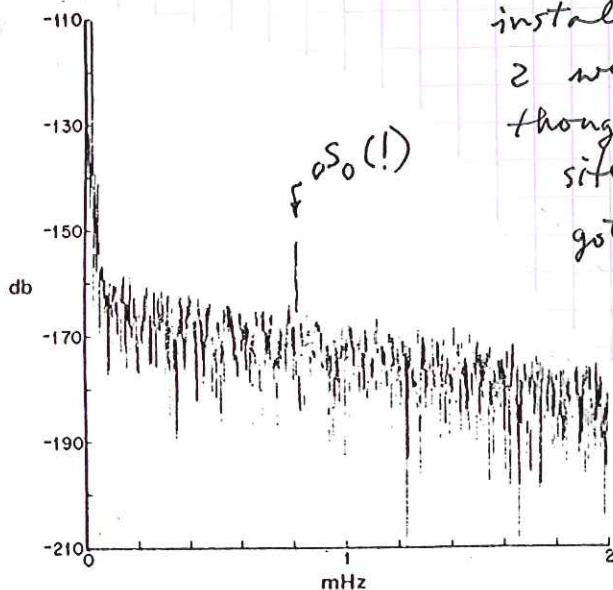


Figure 7. Log integrated power versus time for the weighted stack using windows of 134 hr. The value of Q here is 5800. Error bars are obtained using the work of Dahlen (1976). The unweighted least squares procedure was used.



The operators who were installing the KIP station 2 weeks after the event thought they'd picked a noisy site by mistake until they got home and made a spectrum.

Figure 3. A power spectrum of 120 hr of record from station KIP beginning 18 days after the origin time of the event. Notice the high amplitude of σ_0 while all other modes have died away. Station KIP did not start operation until 2 weeks after the earthquake.

Normal Modes of a SNREI Earth

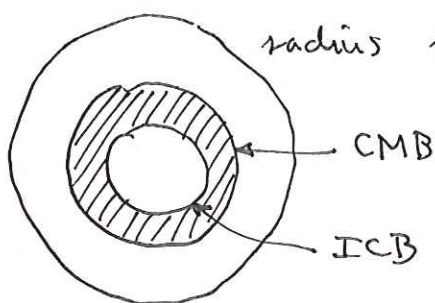
(SNREI = spherical, non-rotating, elastic, isotropic)

Characterized by three functions of radius r only:

$\rho(r)$: density

$\kappa(r)$: incompressibility

$\mu(r)$: rigidity



rigidity $\mu(r) = 0$ in fluid
outer core between
CMB & ICB

To find the modes ω , $s(x)$ we must solve:

$$-\rho \omega^2 s = \nabla \cdot \mathbb{T} \quad \text{in } \Phi$$

$$\hat{n} \cdot \mathbb{T} = \hat{n} \cdot \mathbb{T} = 0 \quad \text{on } \partial\Phi \quad (\text{and } [\hat{r} \cdot \mathbb{T}]_{\pm} = 0$$

$$\text{stress: } \mathbb{T} = \kappa (\nabla \cdot s) \mathbb{I} + 2\mu \delta \quad \text{on CMB \& ICB})$$

$$\text{deviatoric strain: } \delta = \frac{1}{2} [\nabla s + (\nabla s)^T] - \frac{1}{3} (\nabla \cdot s) \mathbb{I}$$

$$\text{tr } \delta = 0$$

Boundary-value problem for a second-order PDE

$$\nabla \cdot \mathbb{T} = \nabla \cdot [\kappa (\nabla \cdot s) \mathbb{I} + 2\mu \delta] \quad \text{i.e.}$$

$$\partial_i T_{ij} = \partial_i [\kappa (\partial_k s_k) \delta_{ij} + 2\mu \delta_{ij}]$$

$$= \partial_j [\kappa (\partial_k s_k)] + \partial_i (2\mu \delta_{ij})$$

Note that $\kappa(r)$ and $\mu(r)$ appear differentiated.

We seek to reduce this PDE system to an ODE system (PDE = partial differential eqn; ODE = ordinary differential eqn) in radius r only. This possible because of spherical symmetry of the Earth model — the problem is separable.

We begin by expressing s in terms of 3 scalars u, V, W :

$$s = \hat{r} u + \nabla_1 V - \hat{r} \times \nabla_1 W$$

The ~~scalars~~ scalars $u(x), V(x), W(x)$ are unique provided we require that

$$\int_{\text{any spherical shell}} V dA = \int_{\text{ditto}} W dA = 0 \quad \text{i.e. average to zero on every spherical shell}$$

∇_1 is the surface gradient on the unit sphere

$$\nabla = \hat{r} \partial_r + \frac{1}{r} \nabla_1$$

$$\nabla_1 = \hat{\theta} \partial_\theta + \hat{\phi} (\sin\theta)^{-1} \partial_\phi$$

If V, W are constant functions of θ, ϕ then

$\nabla_1 V = \nabla_1 W = 0$ — this is the reason for the restriction.

The three scalars ~~u, V, W~~ u, V, W can be expanded in surface spherical harmonics $Y_\ell^m(\theta, \phi)$

These are a known orthogonal basis — they are the eigenfunctions of $\nabla_1 \cdot \nabla_1 = \nabla_1^2$ — the surface Laplacian:

$$\nabla^2 = \frac{1}{r^2} \partial_r^2 + \frac{1}{r^2} \nabla_1^2$$

$$\nabla_1^2 = \frac{1}{\sin\theta} \partial_\theta (\sin\theta \partial_\theta) + \frac{1}{\sin^2\theta} \partial_\phi^2$$

("spherical part" of ∇^2)

$$\nabla_1^2 Y_l^m(\theta, \phi) = -l(l+1) Y_l^m(\theta, \phi)$$

They are orthogonal — and we normalize them — such that

$$\int_{\Omega} Y_l^m Y_{l'}^{m'} dA = \delta_{ll'} \delta_{mm'}$$

→ unit sphere $|r|=1$

In quantum mechanics it is natural to use complex Y_l^m but we shall use real ones.

$$Y_l^m(\theta, \phi) = \cancel{X_l^m(\theta)} \begin{cases} \sqrt{2} \cos m\phi & \text{if } m > 0 \\ 1 & \text{if } m = 0 \\ \sqrt{2} \sin m\phi & \text{if } m < 0 \end{cases}$$

$X_l^m(\theta)$ has $l-|m|$ nodes between 0 and π

↗ $2/|m|$ nodes as a function of ϕ

$$X_l^{-m}(\theta) = (-1)^m X_l^m(\theta)$$

Figure shows $X_l^{10}(\theta)$ compared with an asymptotic approximation valid for $l \gg 1$.

We thus express the displacement in a SNREI model by

$$s(x, t) = \sum_l \sum_m \hat{r} u_l^m(r) Y_l^m(\theta, \phi) \quad (*) \\ + v_l^m(r) \nabla_1 Y_l^m(\theta, \phi) + w_l^m(r) (-\hat{r} \times \nabla_1 Y_l^m(\theta, \phi))$$

vector spherical harmonics defined by:

$$P_l^m = \hat{r} Y_l^m$$

$$B_l^m = \nabla_1 Y_l^m$$

$$C_l^m = -\hat{r} \times \nabla_1 Y_l^m$$

These are orthonormal in the sense

$$\int_{\Omega} P_l^m \cdot P_{l'}^{m'} dA = \delta_{ll'} \delta_{mm'}$$

$$\int_{\Omega} B_l^m \cdot B_{l'}^{m'} dA = l(l+1) \delta_{ll'} \delta_{mm'}$$

$$\int_{\Omega} C_l^m \cdot C_{l'}^{m'} dA = l(l+1) \delta_{ll'} \delta_{mm'}$$

Also any "cross-integral" $\int_{\Omega} P_l^m \cdot B_{l'}^{m'} dA$, etc. = 0.

The divergence of a displacement field of the form $*$ is

$$\nabla \cdot s = \sum_l \sum_m \left[\frac{\partial}{\partial r} u_l^m + \frac{2u_l^m}{r} - \frac{l(l+1)v_l^m}{r} \right] Y_l^m$$

And the curl is no dependence on w_l^m

Every mode is of the form \ast for a single value of l and m — the Y_l^m 's are uncoupled on a spherical Earth. We seek ODE's for u, v, w . There are two ways to proceed, both of which lead to the same result.

1. BRUTE FORCE:

Substitute $s = \hat{r} u Y_l^m + v \nabla_{\theta} Y_l^m + w(-\hat{r} \times \nabla_{\theta} Y_l^m)$
 into ~~$\nabla \cdot \mathbb{T}$~~ $-\rho \omega^2 s = \nabla \cdot \mathbb{T}$
 $\mathbb{T} = \kappa (\nabla \cdot s) \mathbb{I} + 2\mu \delta$

and grind away, using the properties of the Y_l^m 's. This involves substantial algebra. The result is two uncoupled sets of equations, one for the toroidal modes and one for the spheroidal modes

Toroidal modes:

$$\frac{d}{dr} \begin{bmatrix} W \\ T \end{bmatrix} = \begin{bmatrix} r^{-1} & \\ -\rho \omega^2 + \mu(l-1)(l+2)r^{-2} & \mu^{-1} \\ & -3r^{-1} \end{bmatrix} \begin{bmatrix} W \\ T \end{bmatrix}$$

Spheroidal modes:

$$\frac{d}{dr} \begin{bmatrix} u \\ v \\ R \\ S \end{bmatrix} = \begin{bmatrix} -2\lambda \sigma^{-1} r^{-1} & \lambda \sigma^{-1} l(l+1) r^{-1} & \sigma^{-1} & 0 \\ -r^{-1} & r^{-1} & 0 & \mu^{-1} \\ -\rho \omega^2 + 4\mu r^{-2} & -2l(l+1) \mu r^{-2} & 2(\lambda \sigma^{-1} - 1) r^{-1} & l(l+1) r^{-1} \\ -2\mu r^{-1} & -\rho \omega^2 - 2\mu r^{-2} + (l+\mu) l(l+1) r^{-2} & -\lambda \sigma^{-1} r^{-1} & -3r^{-1} \end{bmatrix} \begin{bmatrix} u \\ v \\ R \\ S \end{bmatrix}$$

where $\sigma = \kappa + \frac{4}{3}\mu$, $\lambda = \frac{3\mu\kappa}{\sigma}$, $\lambda = \kappa - \frac{2}{3}\mu$

The associated boundary conditions are:

- toroidal: $T = 0$ on free surface, CMB and ICB
- spheroidal: $S = 0$ on free surface, CMB and ICB
- $R = 0$ on free surface
- $[R]_{\pm} = 0$ on CMB & ICB.

$$\hat{r} \cdot T = \underbrace{R \hat{r} Y_{\ell}^m}_{\text{radial comp.}} + S \nabla_{\hat{r}} Y_{\ell}^m + T (-\hat{r} \times \nabla_{\hat{r}} Y_{\ell}^m)$$

Method 2 - derive from Rayleigh's principle.
Substitute * into the action

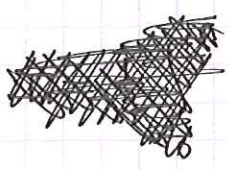
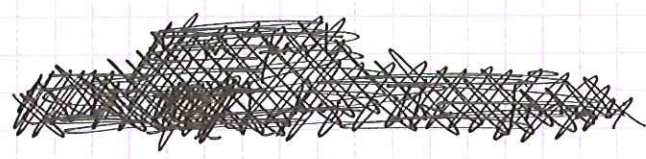
$$I = \frac{1}{2} \int_{\oplus} [\omega^2 \rho s \cdot s - \kappa (\nabla \cdot s)^2 - 2\mu (\sigma : \sigma)] dV$$

and use orthonormality of Y_{ℓ}^m 's. Result is a new action of the form

$$I = \frac{1}{2} \sum_{\ell} \sum_m \int_0^a L_{\ell}^m(r) r^2 dr \quad \leftarrow \begin{array}{l} \text{again no} \\ \text{coupling} \\ \text{each } \ell \end{array}$$

↑ Jacobian

L_{ℓ}^m depends only on $\mu_{\ell}^m, \nu_{\ell}^m, \omega_{\ell}^m$



Get a separate action for each spheroidal & toroidal mode.

Toroidal mode:

$$I = \frac{1}{2} \ell(\ell+1) \int_0^a \left[\rho \omega^2 W^2 - \mu \left(\partial_r W - \frac{W}{r} \right)^2 - \mu(\ell-1)(\ell+2) \frac{W^2}{r^2} \right] r^2 dr$$

kinetic energy
(shear) elastic potential energy of mode

Spheroidal mode:

$$I = \frac{1}{2} \int_0^a \left[\underbrace{\rho \omega^2 (n^2 + l(l+1)V^2)}_{\text{kinetic energy}} - \underbrace{\kappa \left(\partial_r u + \frac{1}{r} (2u - l(l+1)V) \right)^2}_{\text{compressional elastic energy}} \right. \\ \left. - \underbrace{l(l+1)\mu \left(\left(\partial_r V + \frac{n}{r} - \frac{V}{r} \right)^2 + (l-1)(l+2) \frac{V^2}{r^2} \right)}_{\text{shear energy density}} \right] r^2 dr$$

shear energy density — left out a term — see page 62 for correct expression

The toroidal Lagrangian is of the form

$$I_{\text{toroidal}} = \int_b^a L(W, \frac{dW}{dr}) dr$$

$b \leftarrow$ CMB radius — for mantle toroidal modes

Rayleigh's principle asserts that

$$\delta I = \int_b^a \left[\delta W \frac{\partial L}{\partial W} + \frac{d}{dr} (\delta W) \frac{\partial L}{\partial (dW/dr)} \right] dr \\ = \underbrace{\left[\delta W \frac{\partial L}{\partial (dW/dr)} \right]_b^a}_{\text{this gives b.c. } T(b) = T(a) = 0} + \int_b^a \delta W \left[\frac{\partial L}{\partial W} - \frac{d}{dr} \left(\frac{\partial L}{\partial (dW/dr)} \right) \right] dr$$

this gives same eqn as before — one second-order ODE

Ditto for the spheroidal modes

$$I_{\text{spheroidal}} = \int_0^a L(u, v, \frac{du}{dr}, \frac{dv}{dr}) dr$$

In this case get two second-order ODE's and 2 b.c. — one from each of δu and δv — final results same as by BRUTE FORCE method.

Consider a simple example — homogeneous sphere

ρ, κ, μ constant — a marble or shotput or ball bearing

The 2^d order ODE governing the toroidal modes is

$$\left[\frac{1}{r^2} \frac{d}{dr} \left(r^2 \frac{d}{dr} \right) - \frac{l(l+1)}{r^2} + \frac{\omega^2}{\beta^2} \right] W(r) = 0$$

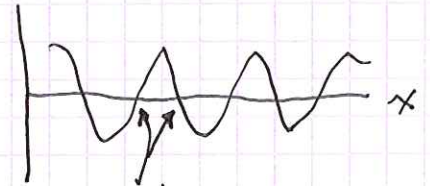
b.c. $T(a) = \mu \left(\frac{dW}{dr} - \frac{W}{r} \right)_a = 0$, where $\beta = \sqrt{\mu/\rho}$ shear wave speed

Solutions are the spherical Bessel functions:

$$W(r) = j_l \left(\frac{\omega r}{\beta} \right) \leftarrow \text{derivative}$$

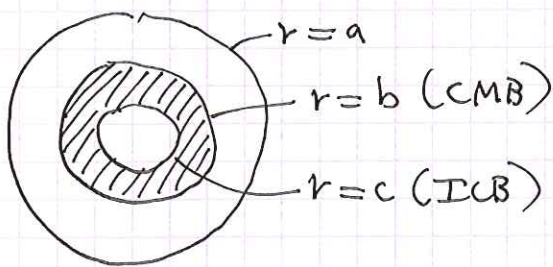
The b.c. $\Rightarrow \left(\frac{\omega a}{\beta} \right) j_l' \left(\frac{\omega a}{\beta} \right) - j_l \left(\frac{\omega a}{\beta} \right) = 0$

Plot ~~of~~ $x j_l'(x) - j_l(x)$



Eigenfrequencies $\omega_l = x_l (\beta/a)$. roots x_l

More generally, for a realistic \oplus model, we use numerical integration. There can be no



toroidal motion in the fluid core where $\mu=0$ (More precisely, any $W(r)$ confined to the fluid core is a trivial solution

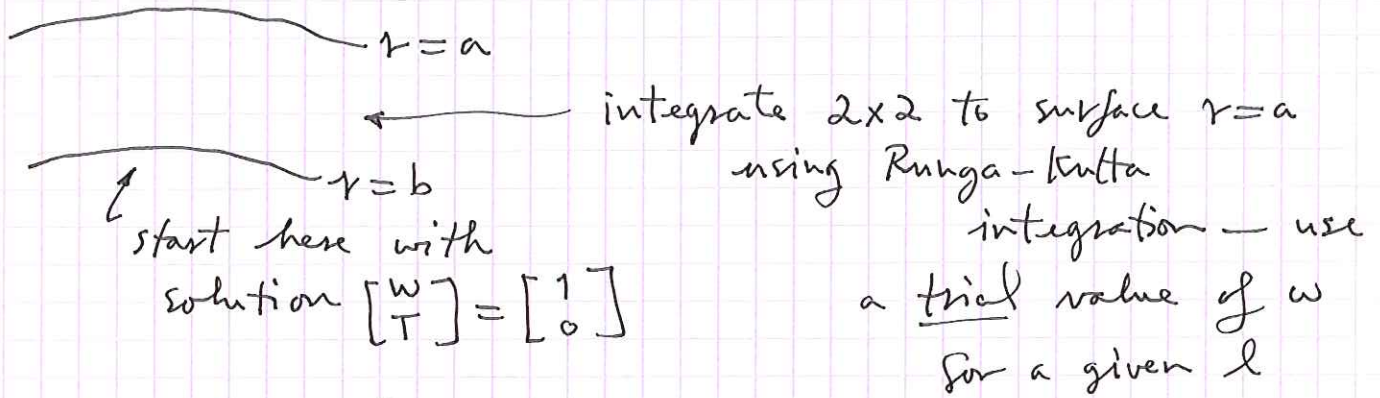
with associated eigenfrequency $\omega=0$ and stress $T = \mu \left(\frac{dW}{dr} - \frac{W}{r} \right) = 0$).

The toroidal modes of the solid inner core are of little interest — can neither be excited by quakes nor observed on the surface. Consider the mantle modes.

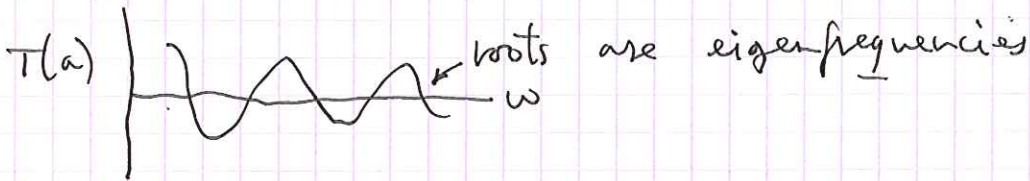
$$\frac{d}{dr} \begin{bmatrix} W \\ T \end{bmatrix} = \begin{bmatrix} 2 \times 2 \text{ matrix} \end{bmatrix} \begin{bmatrix} W \\ T \end{bmatrix}; \quad T(b) = T(a) = 0$$

↑ depends on ω — also nice feature
 does not depend on dp/dr , etc. —

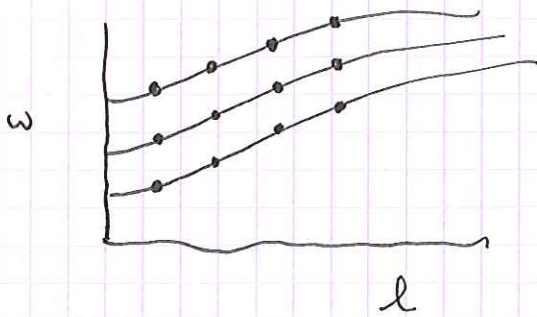
no need to numerically differentiate model — also
 no dependence on κ , only μ — also depends on l .



Now plot $T(a)$ versus ω :



Conventional to plot results on a dispersion diagram.

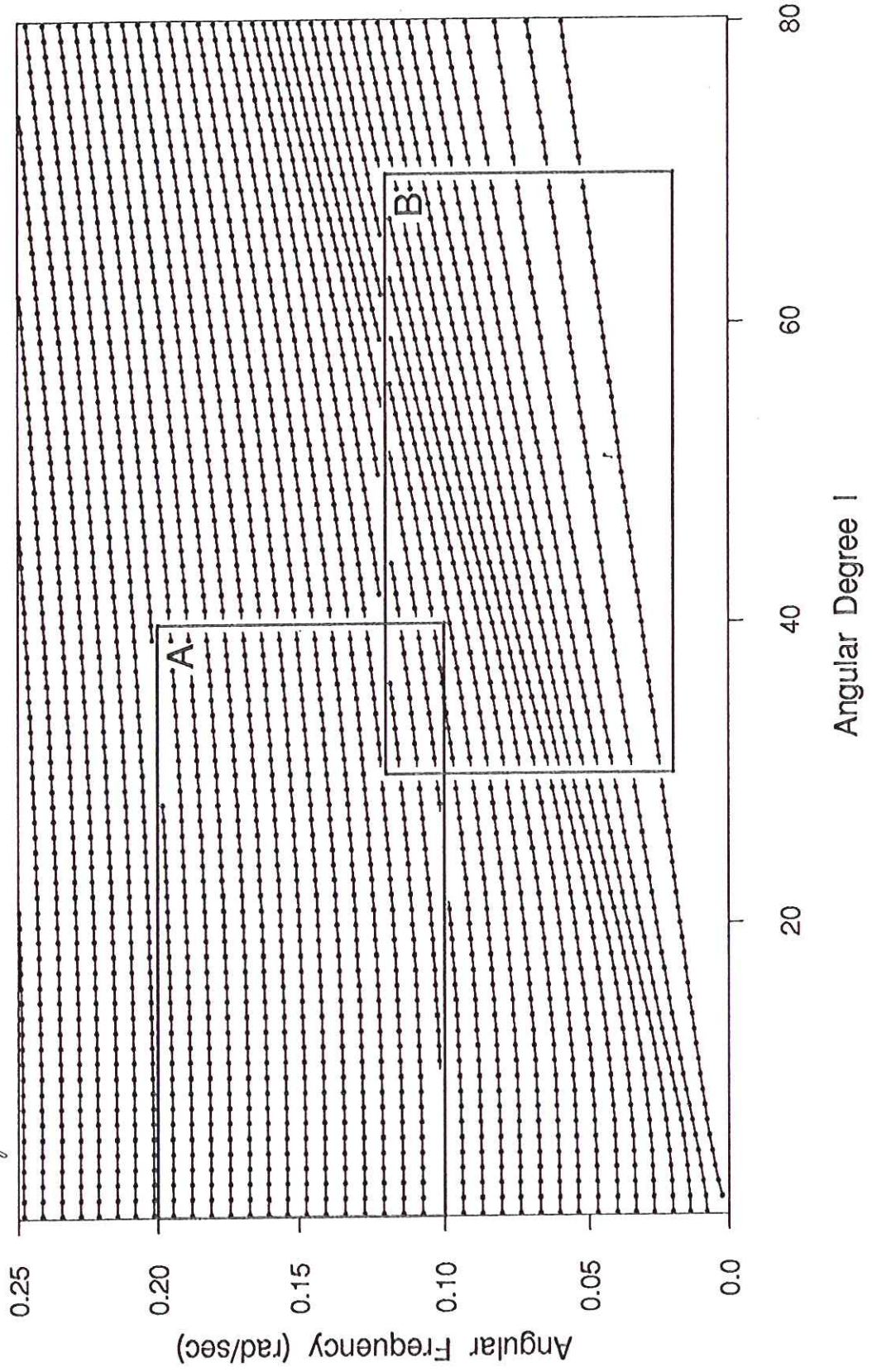


Each dot is a eigenfrequency
 of the Earth. The
 2×2 matrix does not
 depend on m only l — hence
 each frequency is $2l+1$ -
degenerate.

The associated eigenfunctions are of form

$$s = W_{nl}(r) \left[-\hat{r} \times \nabla_{\theta} Y_l^m(\theta, \phi) \right], \quad \underbrace{-l \leq m \leq l}_{2l+1 \text{ modes}}$$

Ignore the boxes A & B - note the regular pattern



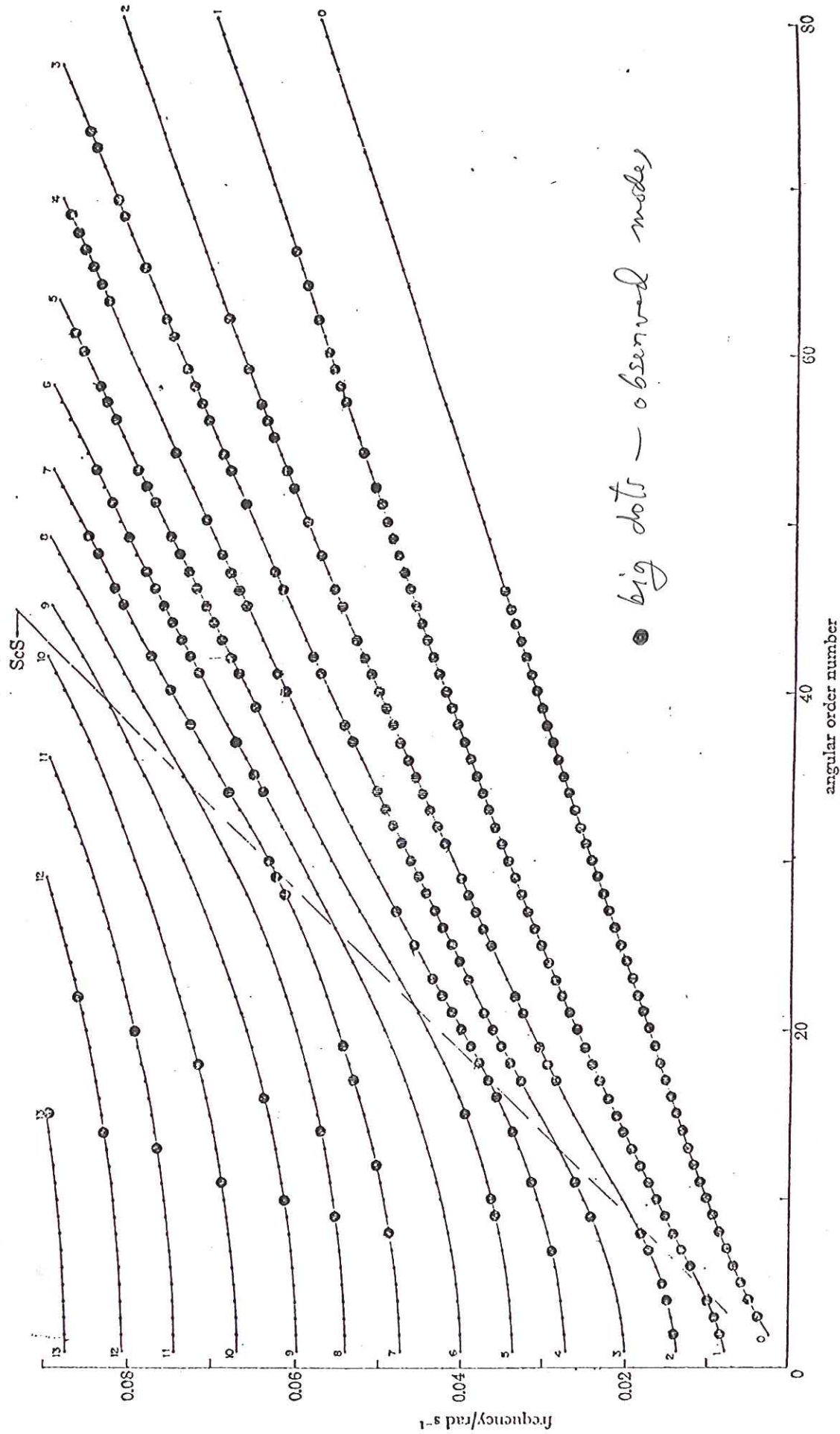
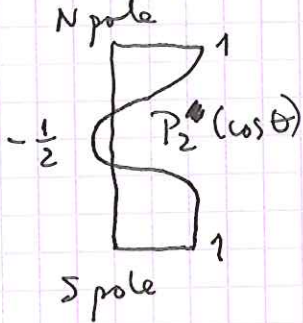


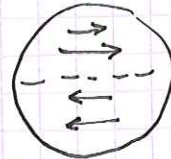
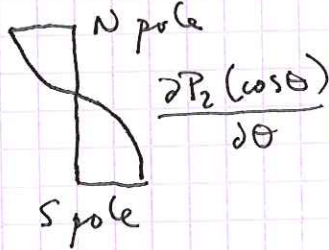
FIGURE 16. Toroidal normal modes in the (ϕ, l) plane. The large dots indicate observed modes used in the inversions. Most of the toroidal overtones identified by Brune & Gilbert (1964) fall outside the range of the figure. The dashed line designated 'ScS' divides the modes into two groups according to the normal mode-body wave analogy: modes to the left of this line correspond to $(\text{ScS})_R$ reflexions, those to the right correspond to mantle S_{II} waves.

$0T_2$ (period $\frac{2\pi}{\omega} \approx 44$ mins) is the gravest toroidal mode — not observed until ~ 2 years ago, following Macquarie Ridge quake — by Walter Zürn & colleagues.

For $m=0$: $Y_2^0(\theta, \phi) = \sqrt{\frac{2\theta+1}{4\pi}} P_2(\cos\theta)$
 Legendre polynomial



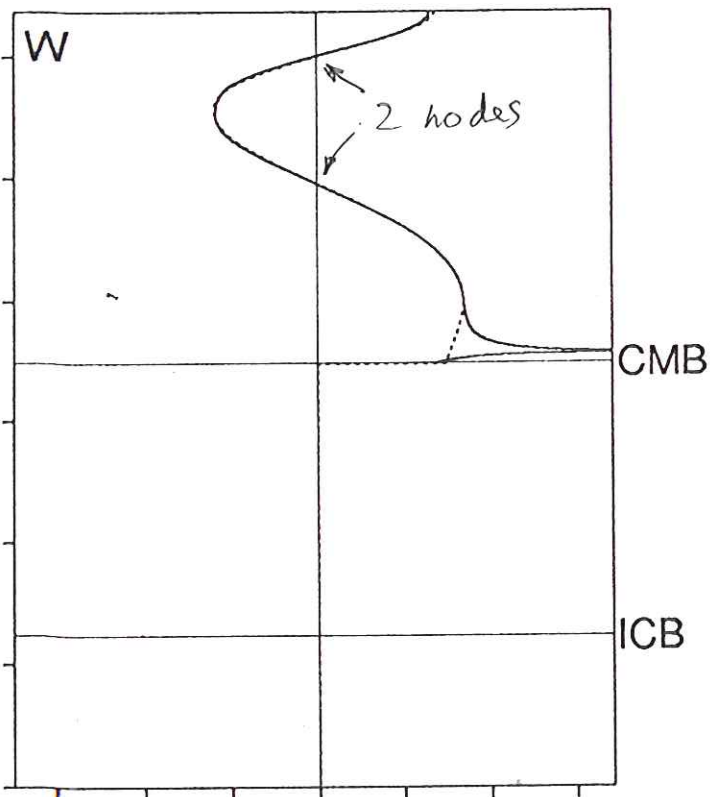
$$e_2^0 = -\hat{\phi} \frac{\partial Y_2^0}{\partial \theta}$$



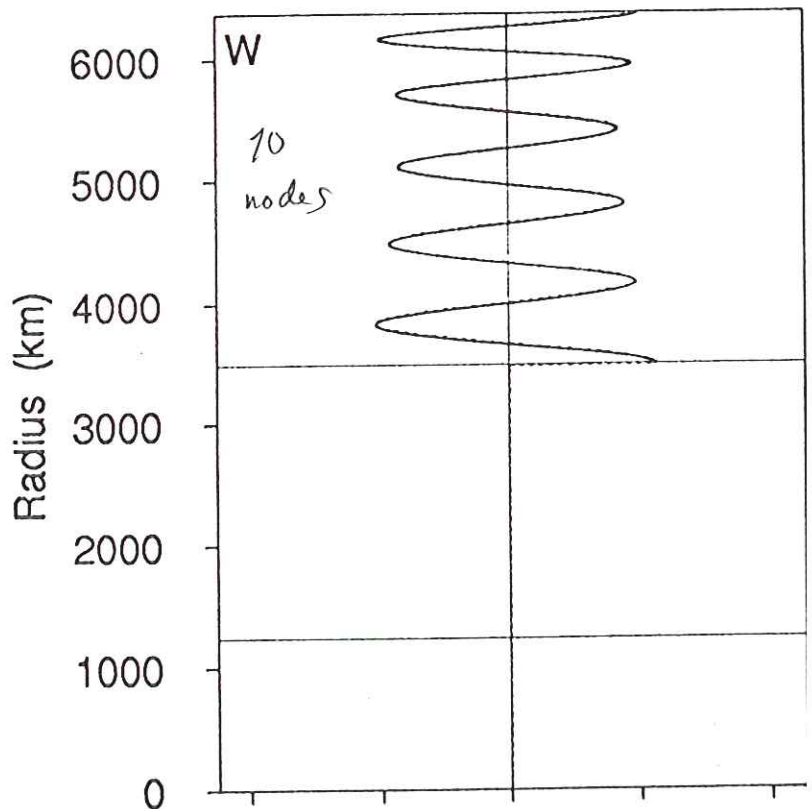
twisting or shearing motion like this.

Every radial eigenfunction ${}_n W_\ell(r)$ has n radial nodes — this a property of Sturm-Liouville system.
 ${}_2 W_{10}$ and ${}_{10} W_{10}$ shown below — ignore the (asymptotic) solid curves for now — model is 7DCGA.

Toroidal Mode ${}_2 T_{10}$



Toroidal Mode ${}_{10} T_{10}$



Spheroidal modes: more generally if we consider the gravitational restoring force as well as the elastic force we must solve a 6×6 system:

$$\frac{d}{dr} \begin{bmatrix} u \\ v \\ R \\ S \\ \phi \\ \psi \end{bmatrix} = \begin{bmatrix} 6 \times 6 \text{ matrix} \\ \text{no dependence on} \\ \rho', \kappa', \mu'; \\ \text{depends on } l \\ \text{and } \omega \end{bmatrix} \begin{bmatrix} u \\ v \\ R \\ S \\ \phi \\ \psi \end{bmatrix}$$

← perturbation in grav. potential
 ← $\frac{d\phi}{dr} + 4\pi G \rho u + \frac{l+1}{r} \phi$

Adding gravity adds 2 eqns — Poisson's equation $\nabla^2 \phi = 4\pi G \delta \rho$ is second-order.

Now three b.c.: $R(a) = 0$
 $S(a) = 0$ } traction
 $\psi(a) = 0$ ← gravity

These are two special cases — in the fluid case the 6×6 system reduces to a 4×4 (since $\mu = 0$).

For the radial modes ($l=0$) reduces to a 2×2 .

To find ω_l we start integration at ~~center~~ of Earth where there are three linearly independent solutions that are finite in the limit $r \rightarrow 0$.

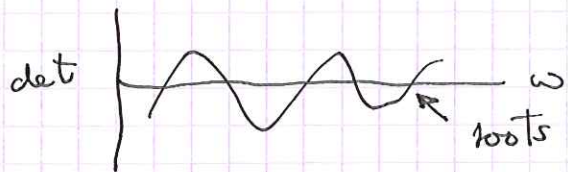
Integrate using R-K each of the three to the surface. The general solution must be ~~the~~

a linear combination:

We want (at $r=a$):

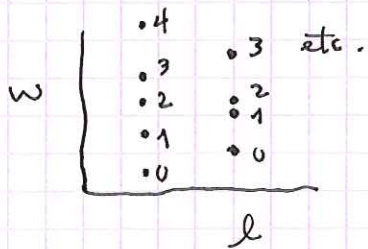
$$a \begin{bmatrix} \text{I} \\ \text{II} \\ \text{III} \end{bmatrix} + b \begin{bmatrix} \text{I} \\ \text{II} \\ \text{III} \end{bmatrix} + c \begin{bmatrix} \text{I} \\ \text{II} \\ \text{III} \end{bmatrix} \quad \begin{bmatrix} R(a) \\ S(a) \\ \psi(a) \end{bmatrix} = \begin{bmatrix} R_{\text{I}} & R_{\text{II}} & R_{\text{III}} \\ S_{\text{I}} & S_{\text{II}} & S_{\text{III}} \\ \psi_{\text{I}} & \psi_{\text{II}} & \psi_{\text{III}} \end{bmatrix} \begin{bmatrix} a \\ b \\ c \end{bmatrix} = \begin{bmatrix} 0 \\ 0 \\ 0 \end{bmatrix}$$

A solution exists only if $\det [3 \times 3] = 0$.

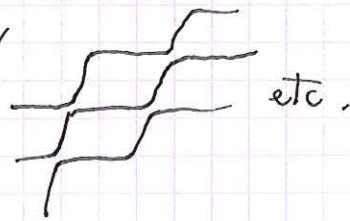


The dispersion diagram ($\omega-l$) is much more complicated for a realistic \oplus model with a solid inner core & fluid outer core than for the toroidal modes.

Nomenclature: for each degree l of Y_l^m one just counts up from the bottom to determine the radial index or overtone number n



When all the ω_{nl} for fixed n are connected the diagram appears to be "terraced"

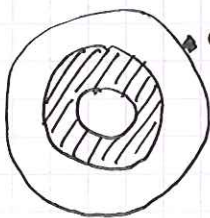


The gravest observed mode is

$0S_2$ — a quintuplet — the "football mode" with a period of ~ 54 minutes $\bigcirc \bigcirc \bigcirc \bigcirc$

It is visibly split by the Earth's rotation.

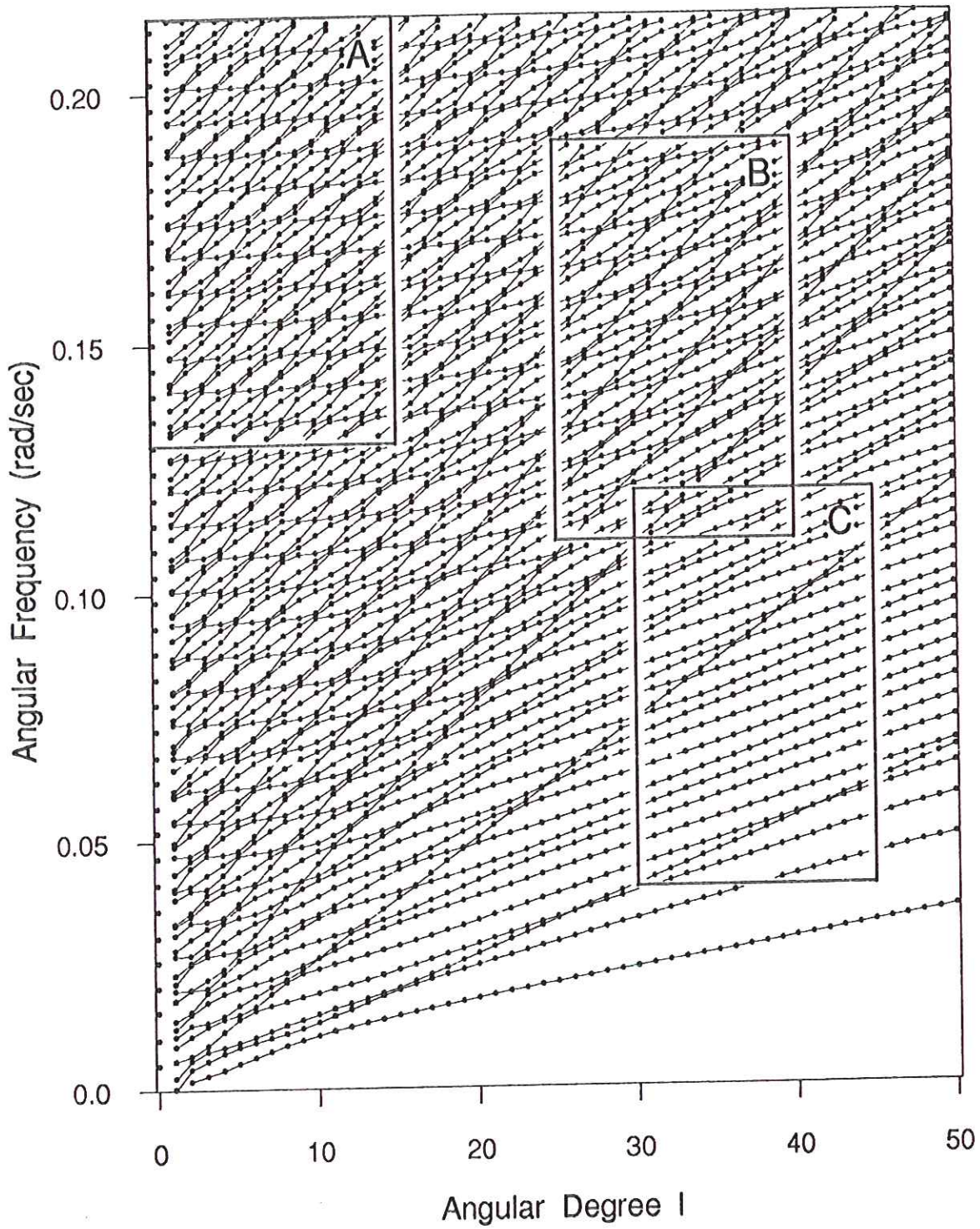
The true gravest elastic mode is $1S_1$ — a triplet — the "Slichter mode" — corresponds to 3 rigid-body translations of solid inner core in fluid — period



can in principle be detected by a gravimeter at surface — but hard to excite by quakes

about 4 hours. The recently claimed "detection" by the Canadian superconducting gravimeter is WRONG!

Ignore Boxes A, B, C



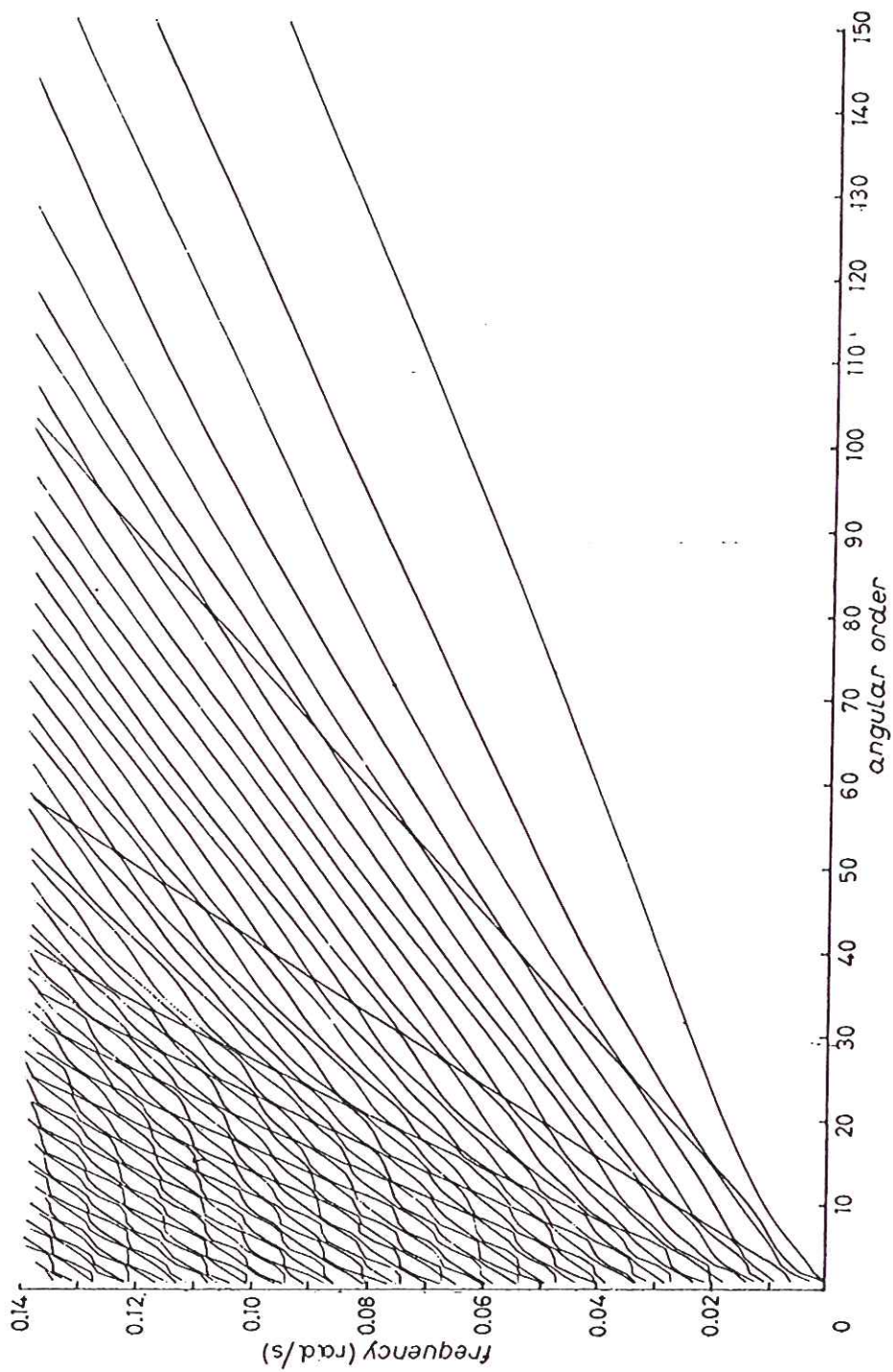


Fig. 3. - (ω, l) diagram for spheroidal, ${}_n S_l$, modes. The points ${}_n \omega_l$ are connected by a continuous line for constant n .

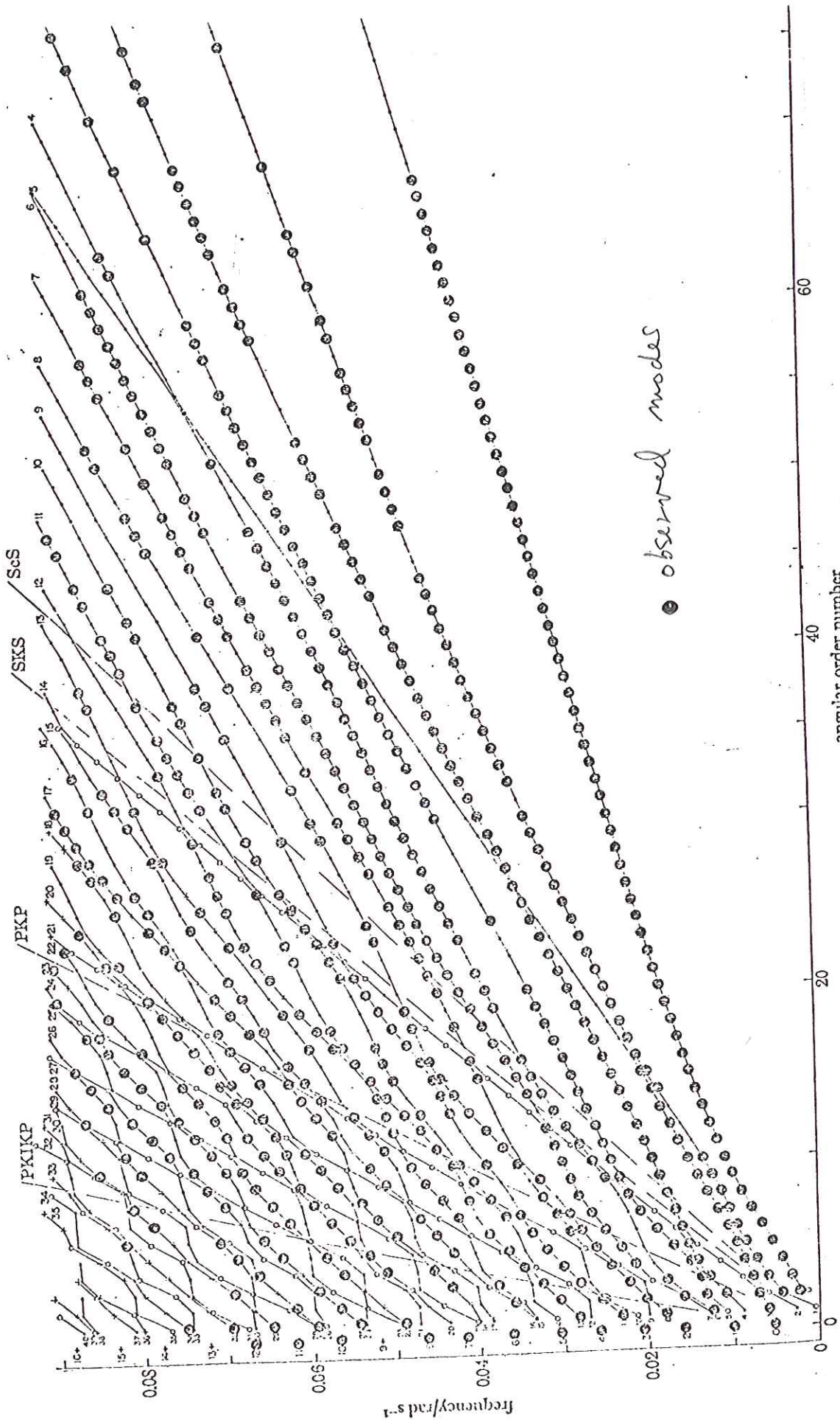


FIGURE 17. Spheroidal normal modes in the (ω, l) plane. The large dots indicate observed modes used in the inversions. For further details we refer the reader to §3 of Alaska II. \bullet , $CE < 0.5$; $+$, $CE \geq 0.5$; \circ core modes.

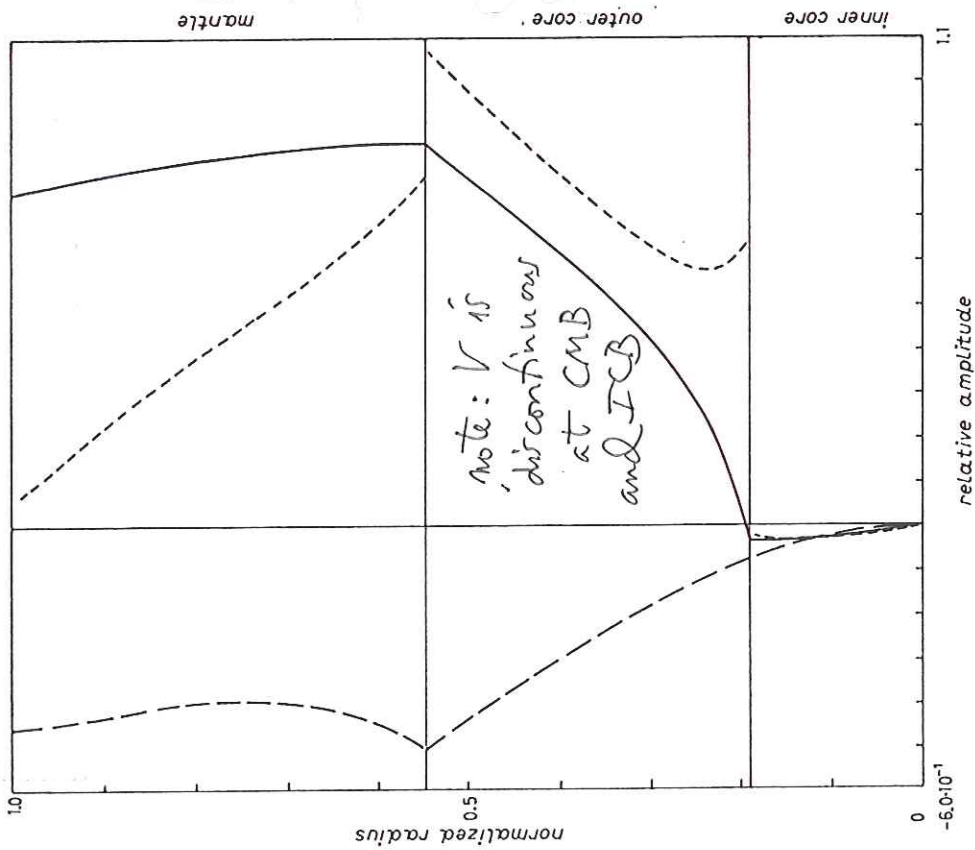


Fig. 4. - The mode S_2 : displacement scalars U (—) and V (---), and perturbation potential Φ (-·-·-).

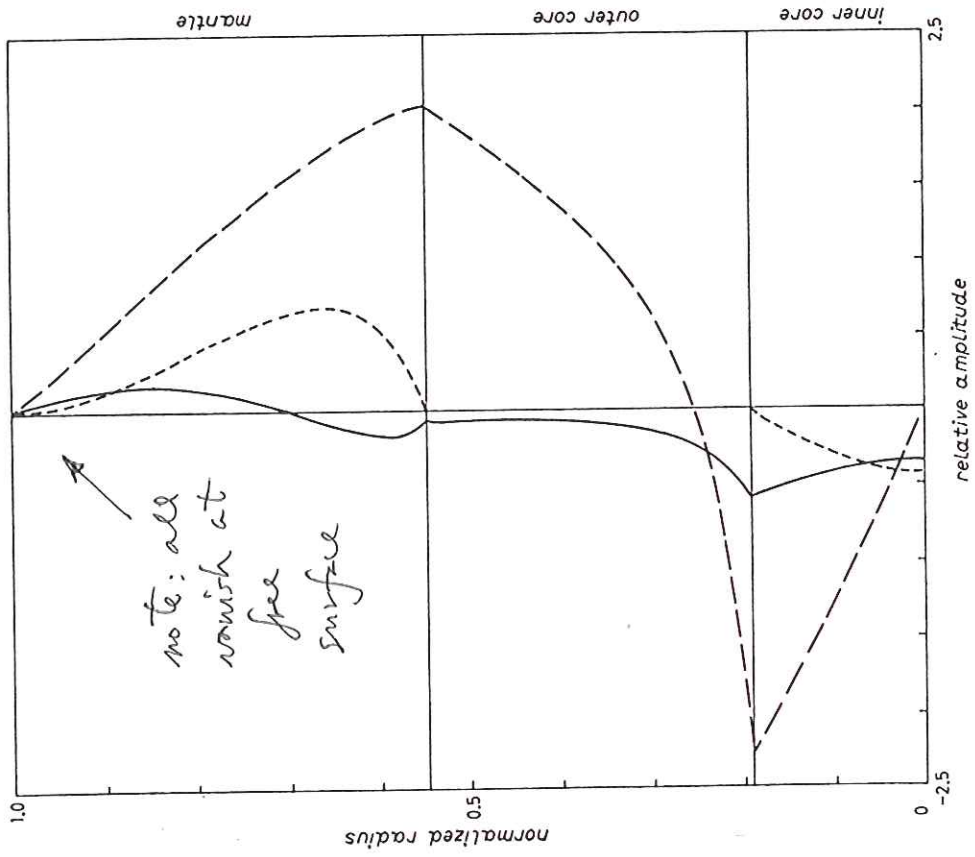


Fig. 5. - The mode S_2 : radial-traction scalars R (—) and S (---), and scalar ψ (-·-·-).

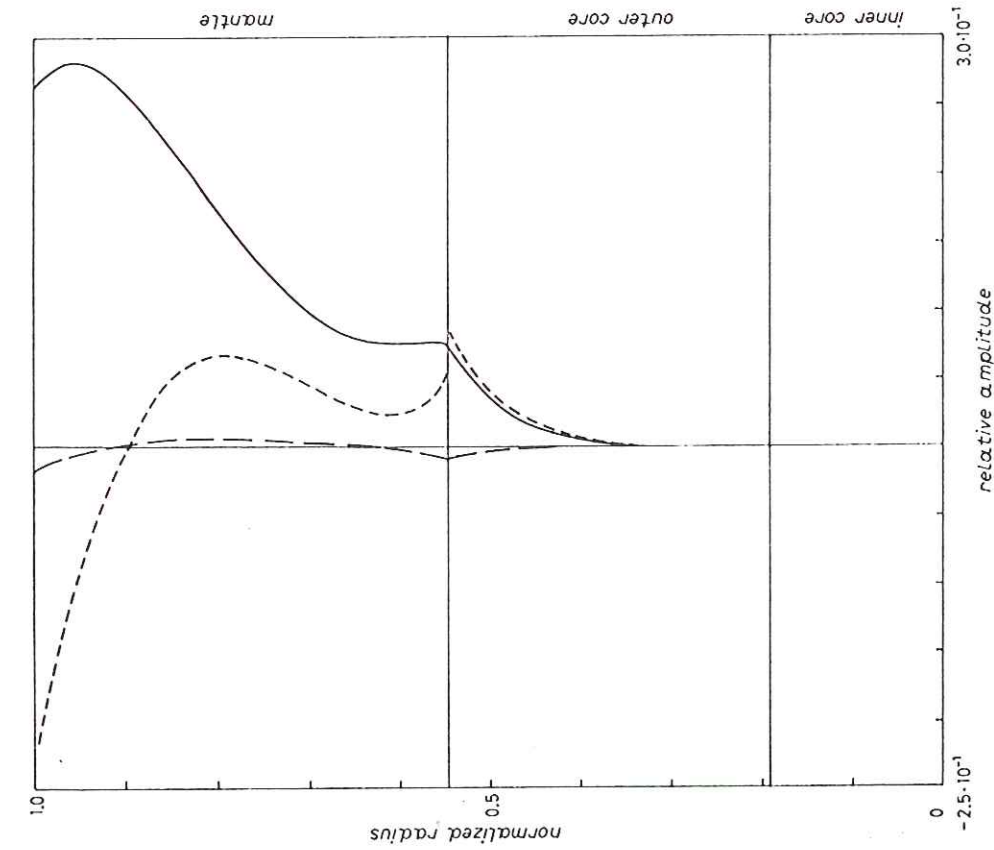


Fig. 7. - The mode ${}_0S_{10}$: displacement scalars U (—) and V (- - -) and perturbation potential Φ (- · - ·).

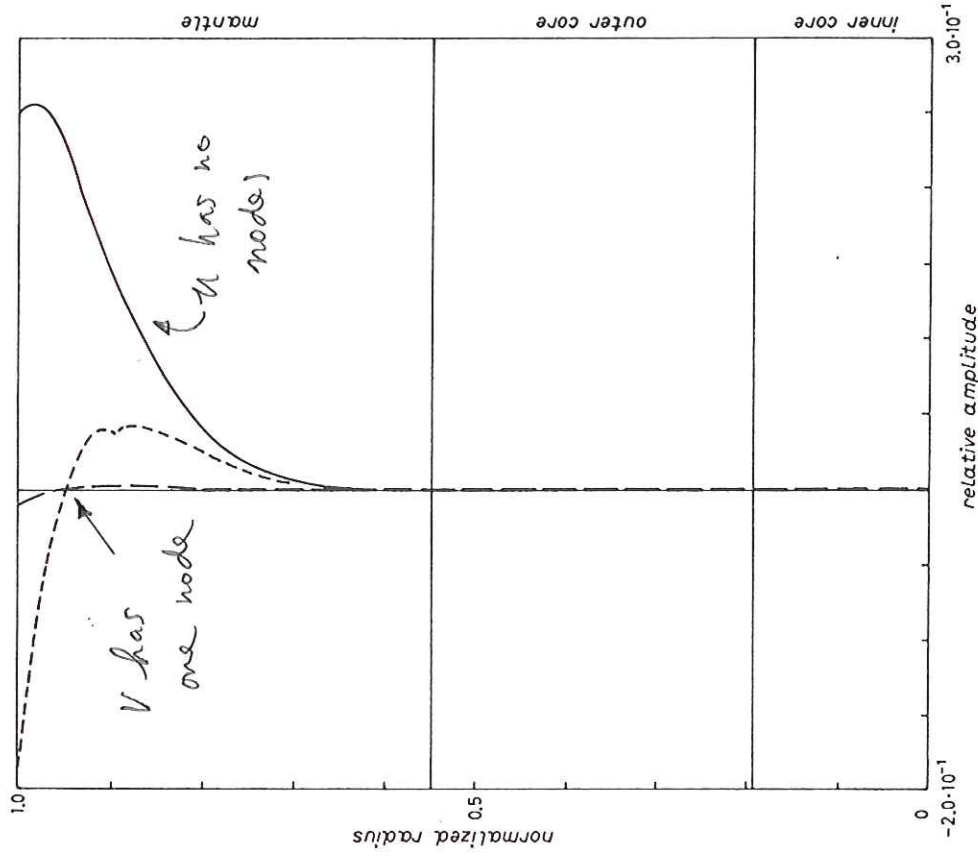


Fig. 10. - The mode ${}_0S_{18}$: displacement scalars U (—) and V (- - -), and perturbation potential Φ (- · - ·).

Surface wave mode

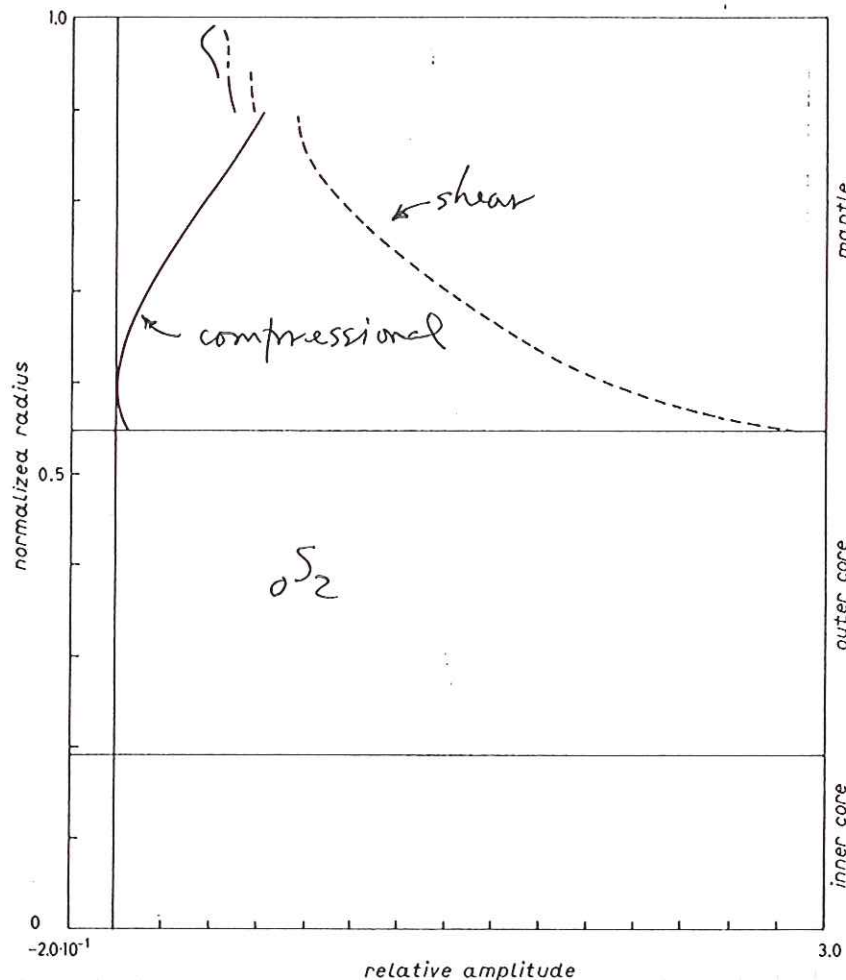
Recall the compressional and shear energy densities are given by

compressional:

$$V_c = \frac{1}{2} \int_0^a \underbrace{\kappa \left[\partial_r u + \frac{1}{r} (2u - l(l+1)V) \right]^2}_{\text{density}} r^2 dr$$

shear

$$V_s = \frac{1}{2} \int_0^a \underbrace{\mu \left[\frac{1}{3} (2\partial_r u - \frac{2u}{r} + \frac{l(l+1)V}{r})^2 + l(l+1) \left(\partial_r V + \frac{u}{r} - \frac{V}{r} \right)^2 + l(l+1)(l-1)(l+2) \frac{V^2}{r^2} \right]}_{\text{density}} r^2 dr$$



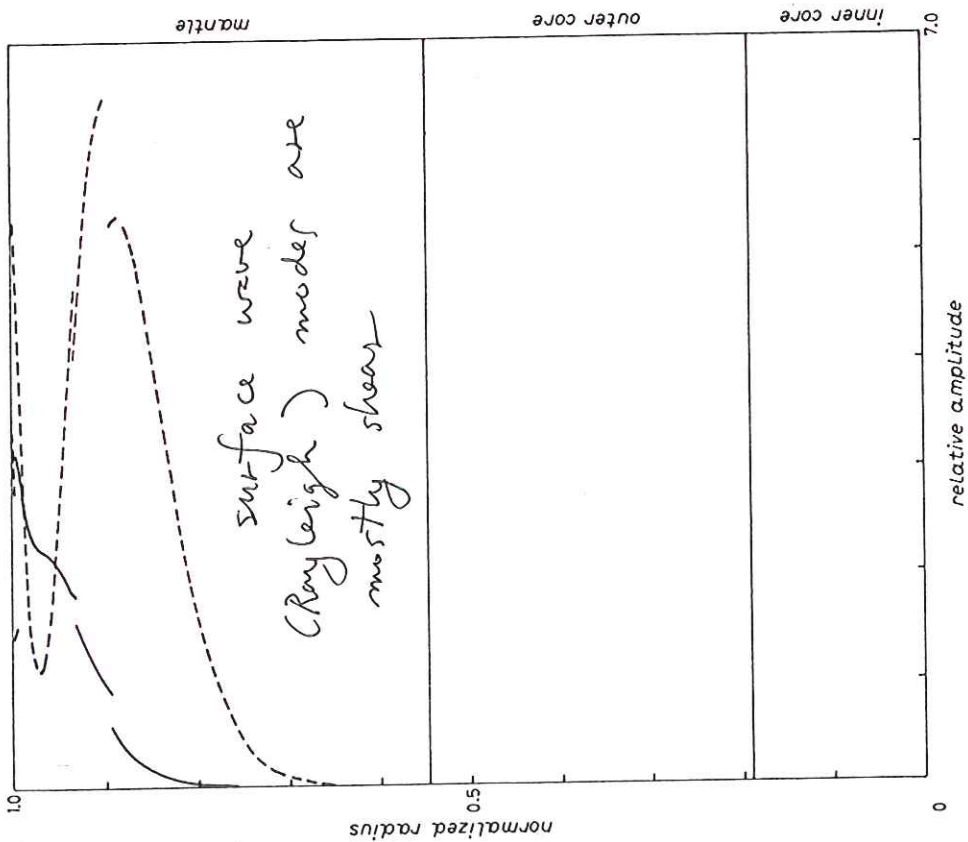


Fig. 12. - The mode ${}_0S_{19}$: compressional-energy density (—) and shear energy density (---).

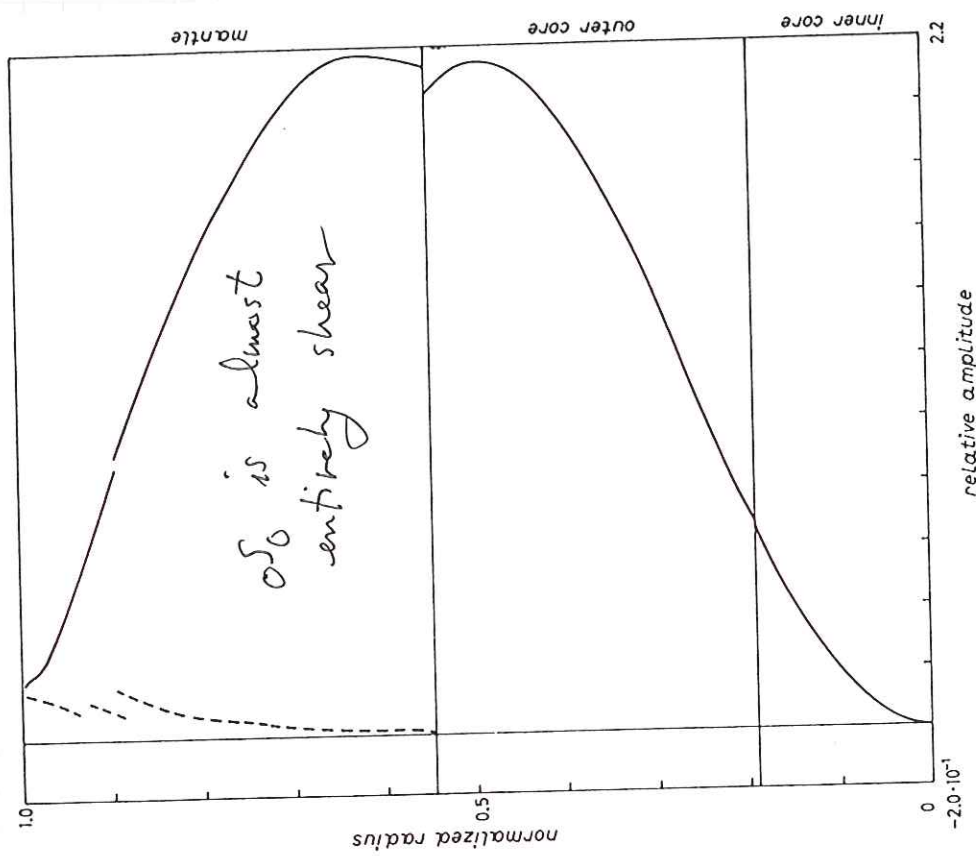
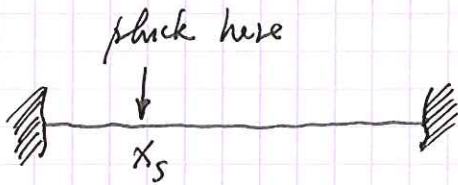


Fig. 13. - Compressional (—) and shear (---) energy densities for ${}_0S_0$.

Mode - Ray Duality

We consider next the correspondence between normal modes or standing waves and travelling body waves.

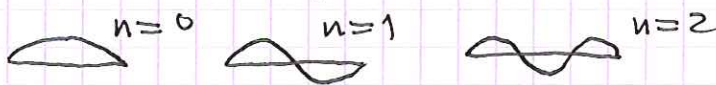
Analogy: a violin string 

The response can be written as a sum of standing waves:

$$u(x,t) = \sum_{n=1}^{\infty} \left(\frac{1}{\rho c n \pi} \right) \sin\left(\frac{n\pi x_s}{L}\right) \sin\left(\frac{n\pi x}{L}\right) \sin\left(\frac{n\pi c t}{L}\right)$$

Note: reciprocity - $x \leftrightarrow x_s$

$c = \sqrt{T/\rho}$ wave speed



$\rho = \text{density}$, $T = \text{tension}$

$L = \text{length}$

Or as a sum of propagating pulses

$$u(x,t) = \frac{1}{2\rho c} \sum_{j=1}^{\infty} e^{-iN_j \pi} H(t - d_j/c)$$

The distance travelled by the j^{th} pulse is d_j .
Each reflection off the end gives rise to a phase change of π

$$d_1 = |x - x_s|$$

$$N_1 = 0$$

$$d_2 = x + x_s$$

$$N_2 = 1$$

$$d_3 = 2L - (x + x_s)$$

$$N_3 = 1$$

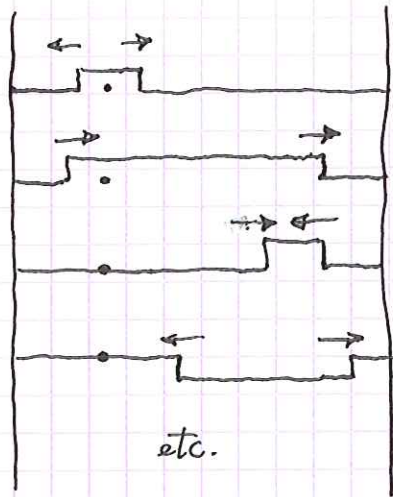
$$d_4 = 2L - |x - x_s|$$

$$N_4 = 2$$

$$d_{j+4} = 2L + d_j$$

$$N_{j+4} = N_j + 2$$

Snapshots:



just after strike at point.
 after reflection off left wall
 after reflection off right wall
 after two pulses have passed
 through each other at
 "antinode"
 etc.

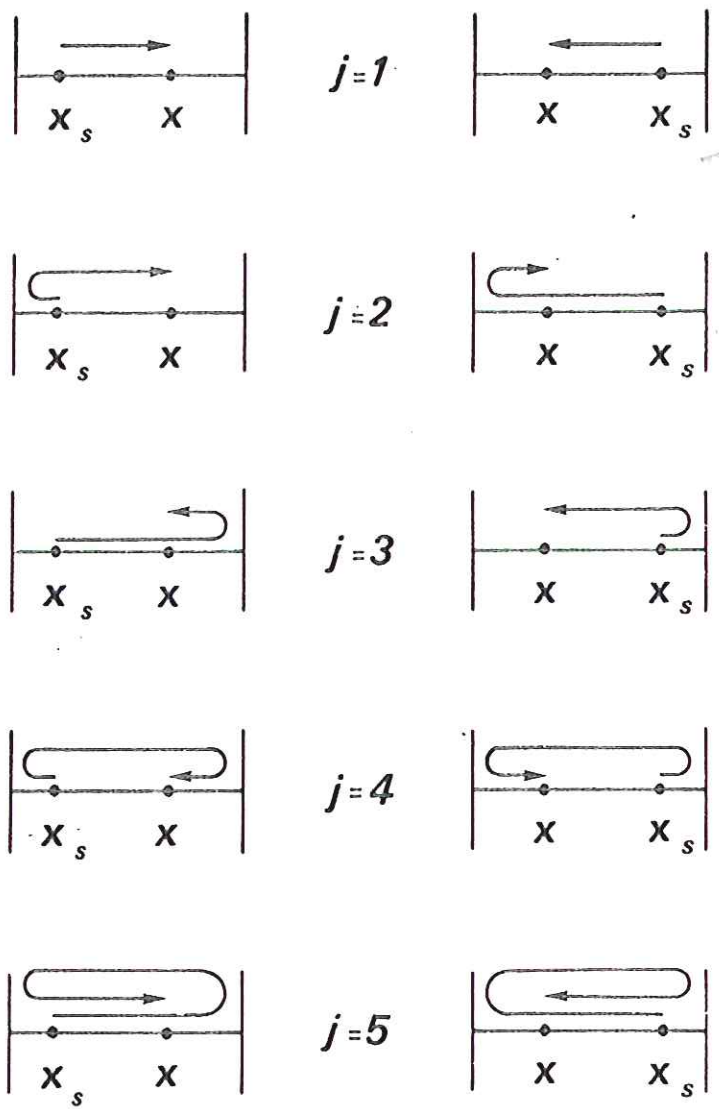
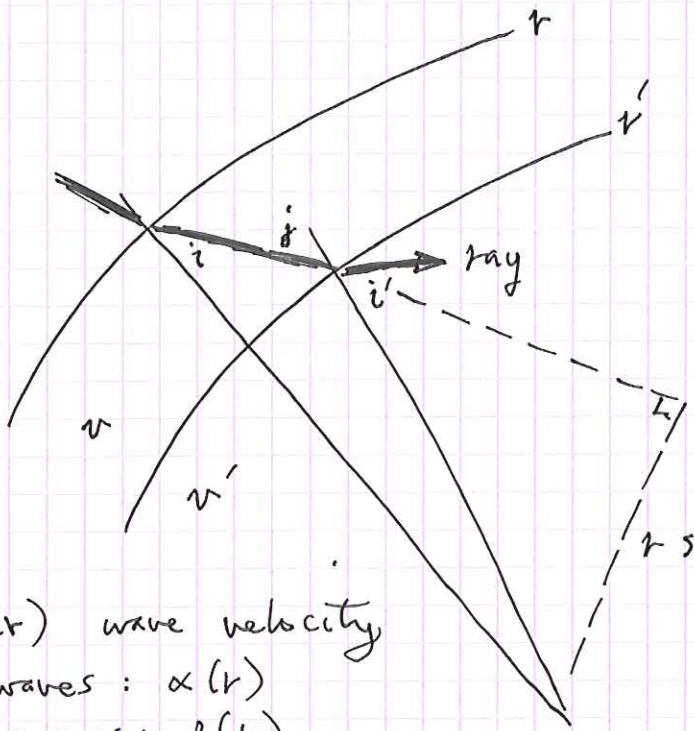


FIG. 1. The convention used for labeling waves on a string. The travel paths for the waves labeled by $j = 1$ to 5 are shown: *left*, if $x_s < x$, *right*, if $x_s > x$. In both cases, $j = 2$ is reflected once at $x = 0$ and $j = 3$ is reflected once at $x = 1$. In general, the index j does not denote the order of arrival.

We begin with a quick review of ray theory



Snell's law:

$$\frac{\sin j}{v} = \frac{\sin i'}{v'}$$

Multiply by r'

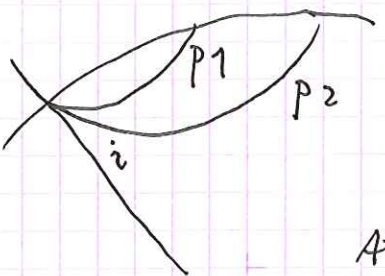
$$\frac{r' \sin j}{v} = \frac{r' \sin i'}{v'}$$

$$r \sin i = r' \sin i'$$

Thus: $\frac{r \sin i}{v} = \frac{r' \sin i'}{v'}$

$v(r)$ wave velocity
 P waves: $\alpha(r)$
 S waves: $\beta(r)$

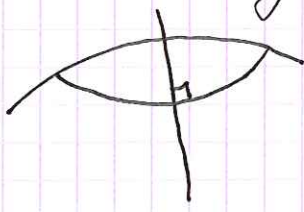
The ray parameter $p = \frac{r \sin i}{v}$ is constant along a ray



$$p_2 < p_1$$

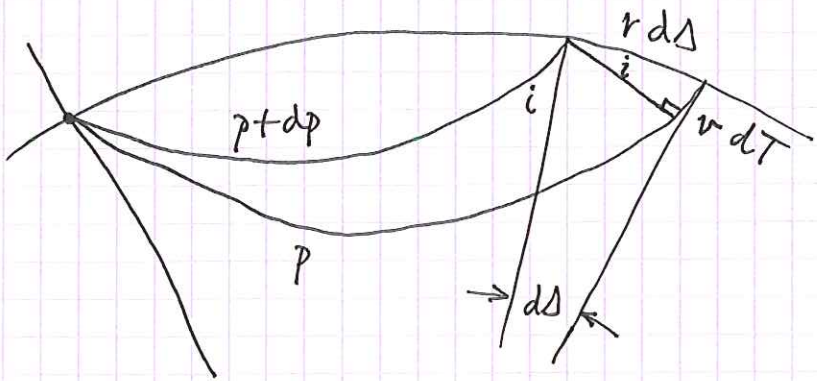
units of p : seconds per radian

At bottoming point of ray $i = 90^\circ$



$$p = r_p / v(r_p)$$

r_p = bottoming depth

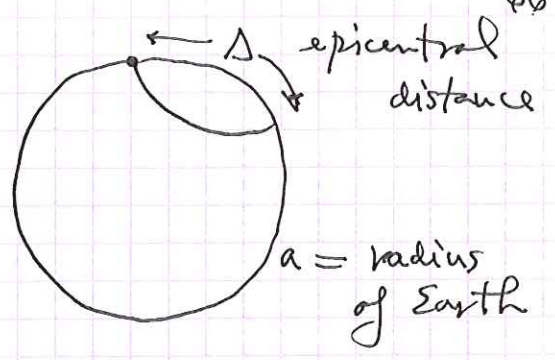
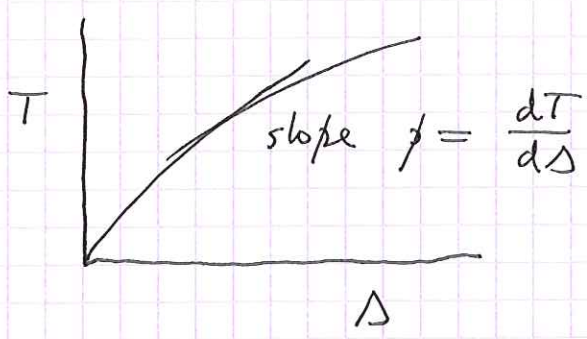


$$\sin i = \frac{v dT}{r d\Delta}$$

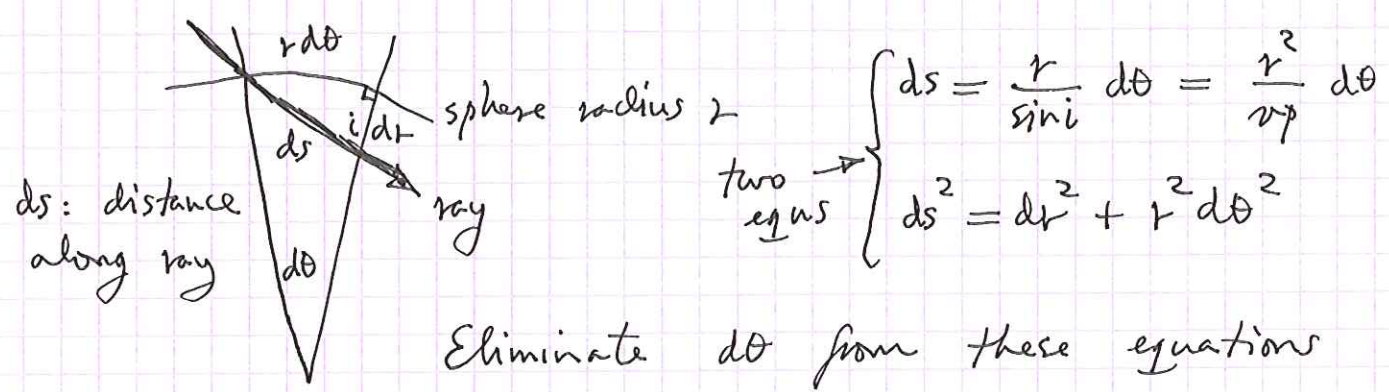
$$\frac{r \sin i}{v} = \frac{dT}{ds}$$

$p = \frac{dT}{ds}$, slope of travel time curve

Consider 2 rays p and $p+dp$ leaving same source



The forward problem of ray theory is to calculate T versus Δ for a given velocity model $v(r)$



Eliminate $d\theta$ from these equations

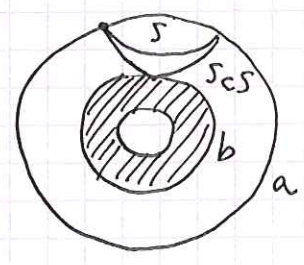
$$dT = \frac{ds}{v} = \pm \frac{dr}{v^2 \sqrt{v^{-2} - p^2 r^{-2}}}$$

$$T = \int_{\text{ray}} dT$$

sign depends on whether ray is going up or down

For a turning ray: P or S

$$T = 2 \int_{\text{turning pt. } r_p}^a \frac{dr}{v^2 \sqrt{v^{-2} - p^2 r^{-2}}}$$



For a reflected ray: Pcp or ScS

$$T = 2 \int_{\text{CMB } b}^a \frac{dr}{v^2 \sqrt{v^{-2} - p^2 r^{-2}}}$$

This gives $T(p)$ for a ray of parameter P .

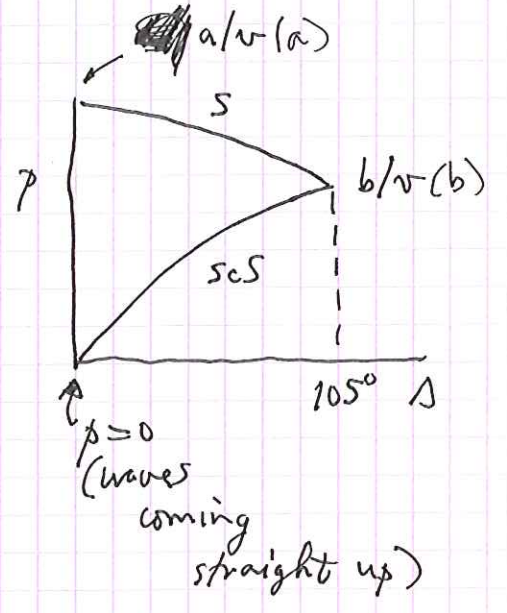
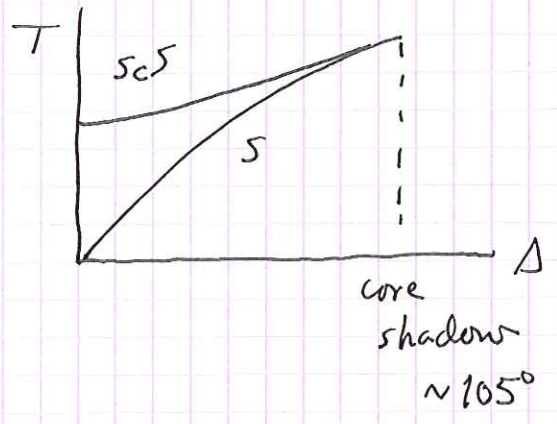
If instead eliminate ds from 2 eqns find

$$ds = \pm \frac{p}{r^2 \sqrt{v^{-2} - p^2 r^{-2}}}$$

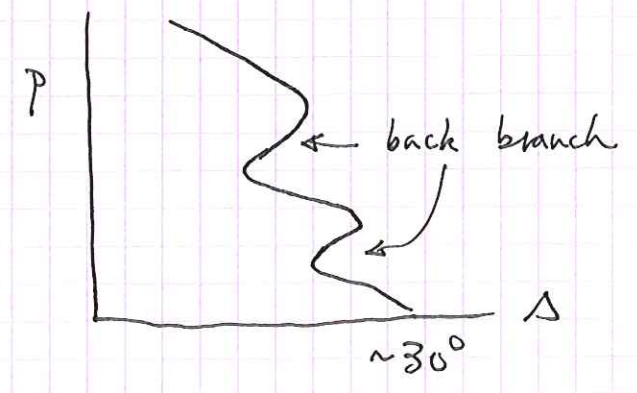
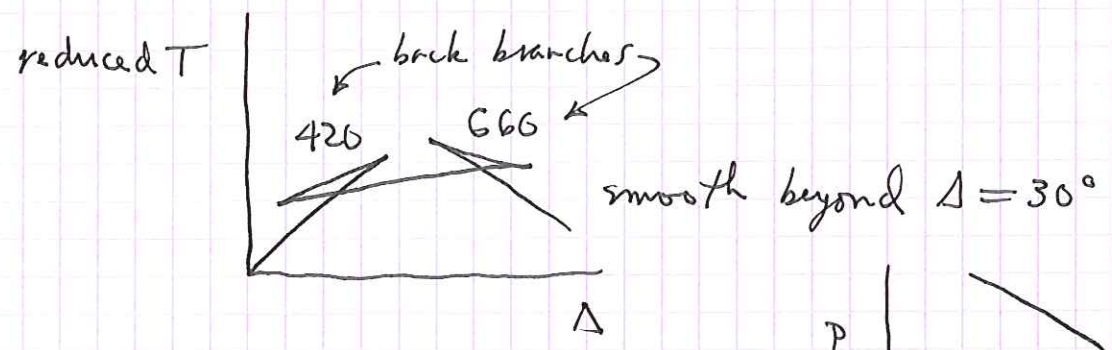
$$\Delta(p) = \int_{ray} ds$$

$$\Delta = 2 \int_{r_p \text{ or } b}^a \frac{p dr}{r^2 \sqrt{v^{-2} - p^2 r^{-2}}}$$

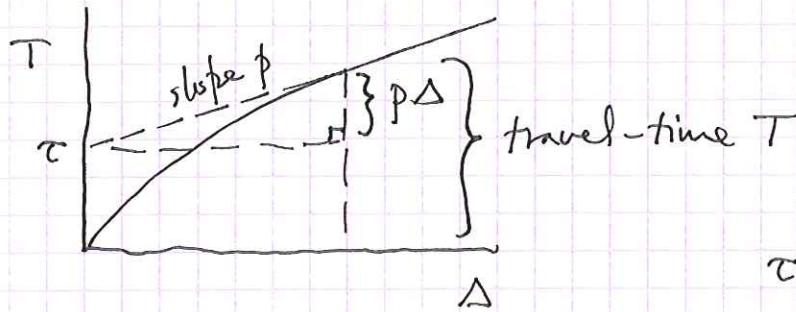
Given $T(p)$ & $\Delta(p)$ can find $T(\Delta)$



The steep velocity gradients in the upper mantle give rise to travel-time trifurcations.



The intercept time τ is defined by



$$\tau = T - p\Delta$$

This has a number of nice properties.

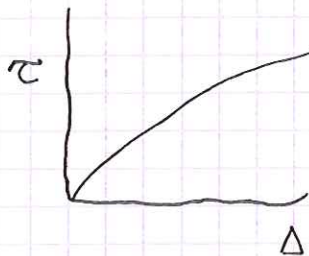
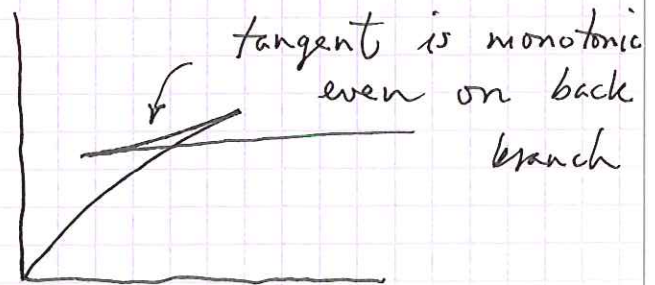
By combining formulae for $T(p)$ and $d(p)$ find

$$\tau(p) = 2 \int_{r \text{ or } b}^a \sqrt{v^{-2} - p^2 r^{-2}} dr$$

↑ no singularity

Consider a triplication:

Hence $\tau(\Delta)$ has no triplication



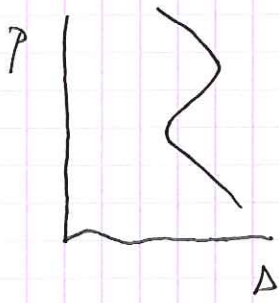
Consider $\frac{d\tau}{dp} = \frac{d}{dp} (T - p\Delta)$

$$= \frac{dT}{dp} - \Delta - p \frac{d\Delta}{dp}$$

$$\frac{d\tau}{dp} = -\Delta$$

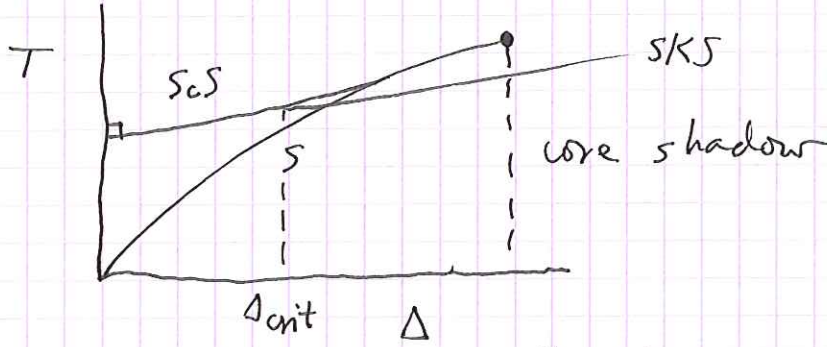
$$= \frac{dT}{dp} - \Delta - \frac{dT}{d\Delta} \frac{d\Delta}{dp} = -\Delta$$

↑ cancel ↑

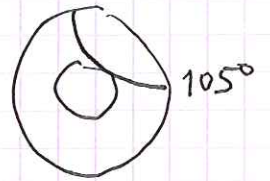
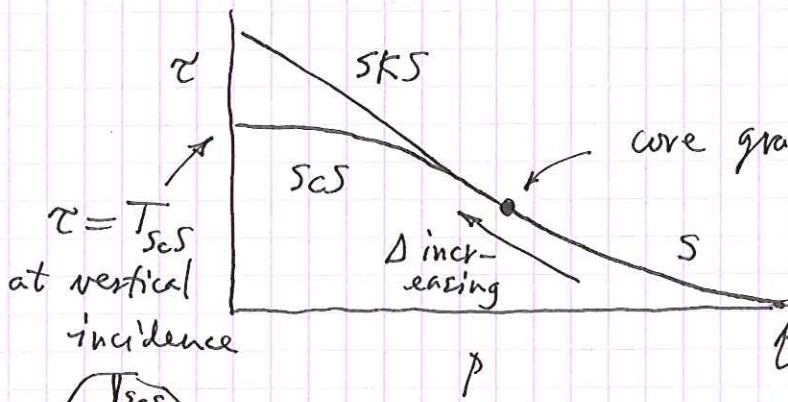


$p(\Delta)$ is triple-valued but $\Delta(p)$ is always single-valued

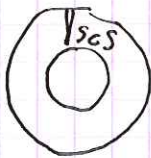
Thus $\tau(p)$ is monotonically decreasing and single-valued.



The $\tau(p)$ curve looks like: *for SH waves*



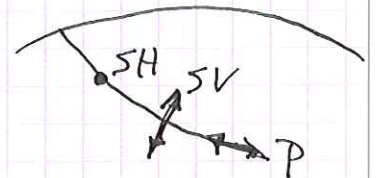
$\tau = T_{ScS}$ at vertical incidence



$$\frac{d\tau}{dp} = -\Delta = 0 \text{ at } p = \frac{a}{\beta_{crust}}$$

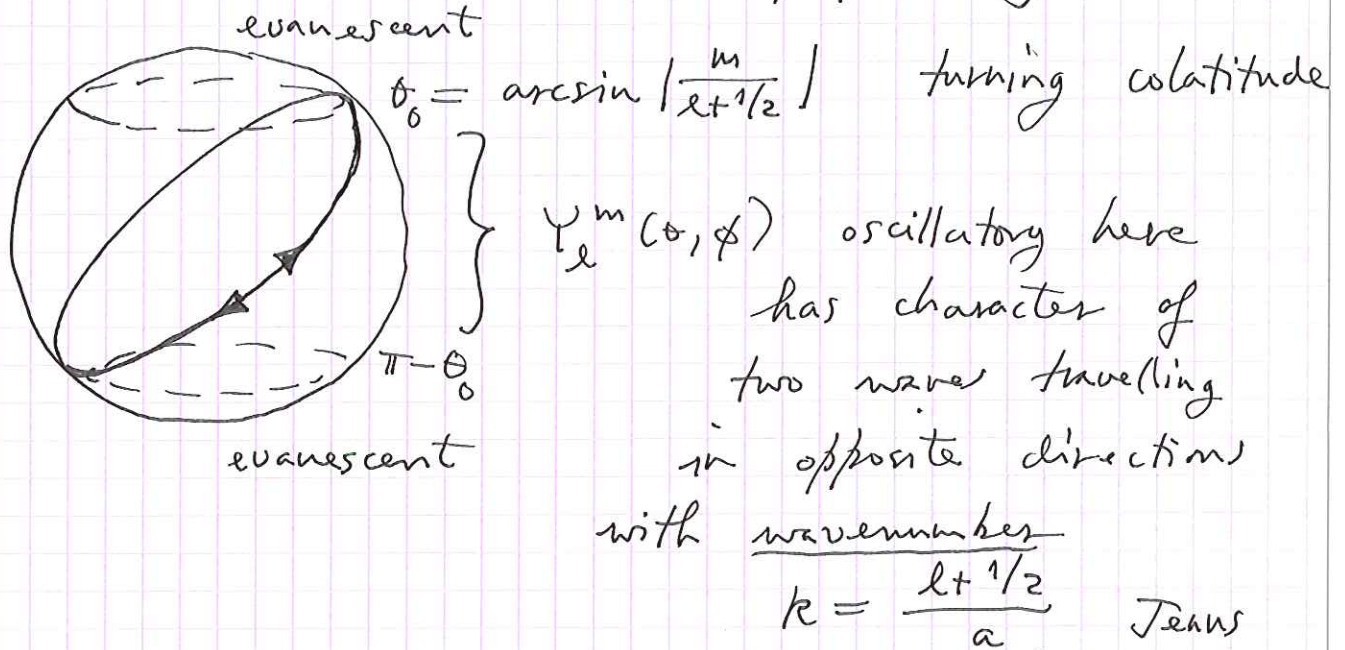
We consider now the correspondence between the toroidal modes & SH body waves

mode	body wave	surface wave
toroidal	SH	Love
spheroidal	P-SV	Rayleigh



The Jean's Relation (Sir James Jeans ~ 1920's) gives the asymptotic wavenumbers of the waves equivalent to the modes n_{TE} or n_{SE} .

For $l \gg 1$ can show that, asymptotically:



A special case ($m=0$):

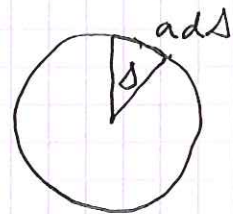
$$Y_l^0(\theta) \sim \frac{1}{\pi} (\sin \theta)^{-1/2} \cos \left[(l + \frac{1}{2})\theta - \frac{\pi}{4} \right] \text{ for } l \gg 1.$$

($\theta_0 = 0$ in this case)

The phase velocity is $\frac{\omega}{k} = \frac{\omega a}{l + 1/2}$

Can also write the phase velocity in terms of the ray parameter p :

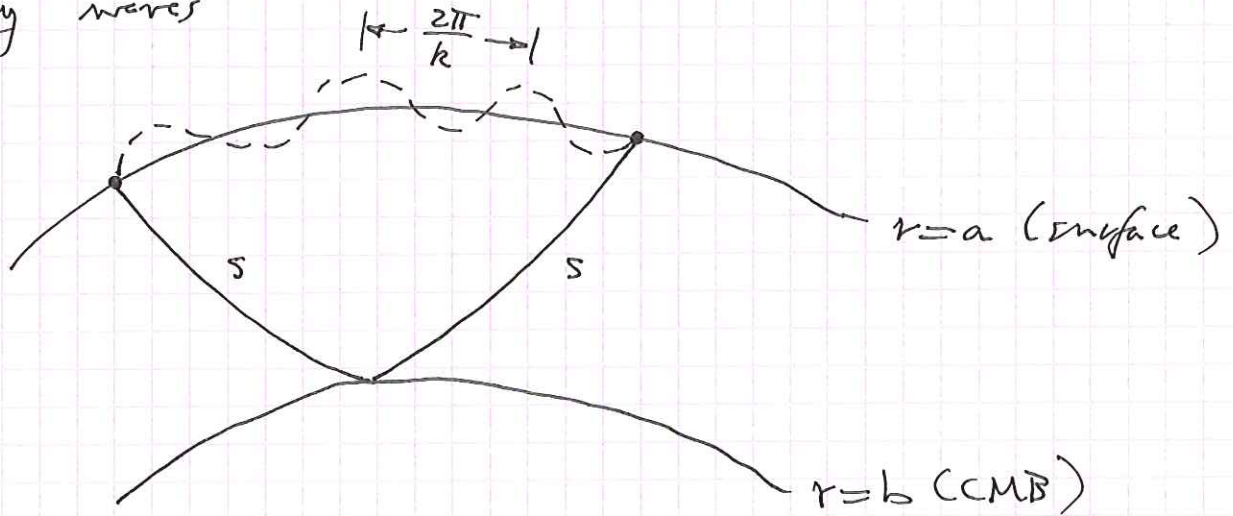
$$\frac{\omega a}{l + 1/2} = \frac{a \, d\Delta}{dT} = \frac{a}{p}$$



Comparing, we find:

$$\boxed{\omega p = l + 1/2}$$

We can obtain a simple asymptotic formula for the toroidal eigenfrequencies using a physical constructive interference argument. We regard the mode as standing wave as the result of the constructive interference of propagating STH body waves



The (dotted ---) phase variation along the surface is simply $\omega p \Delta$. The phase variation along the s ray is ωT_{sCS} . The constructive interference condition is

$$\omega T = \omega p \Delta + 2n\pi \quad (n = 0, 1, 2, \dots)$$

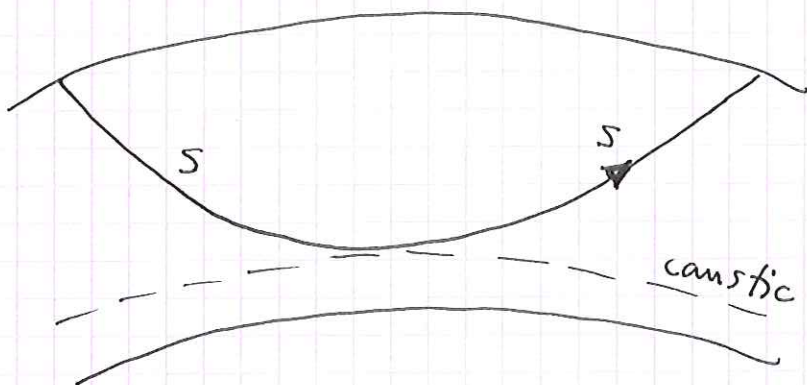
$$\boxed{\omega T = 2n\pi}$$

This gives 2 "semi-classical" quantization conditions to determine ω_l :

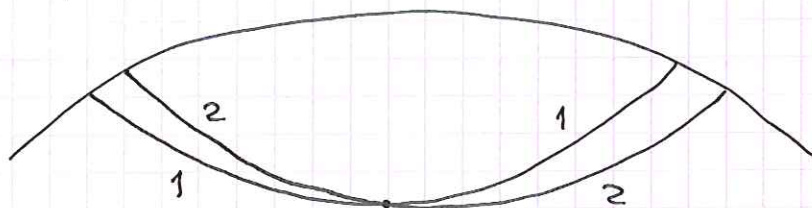
$$\omega p = l + 1/2 \quad \leftarrow \text{half-integer comes from}$$

$$\omega T(p) = 2n\pi \quad \text{polar (caustic) phase shift}$$

For larger P the ray turns rather than reflects:



The turning radius r_p is a caustic or envelope of the family of all rays of ray parameter p :



↑ rays 1 and 2 cross at the caustic

As a result there is a $\pi/2$ phase shift upon turning —

amplitude $\sim \frac{1}{\sqrt{\text{width}}}$ — raytube width $\rightarrow 0$
 changes sign
 $\sqrt{-1} = e^{i\pi/2}$

In this case we find

$$\omega T - \frac{\pi}{2} = \omega p \Delta + 2n\pi$$

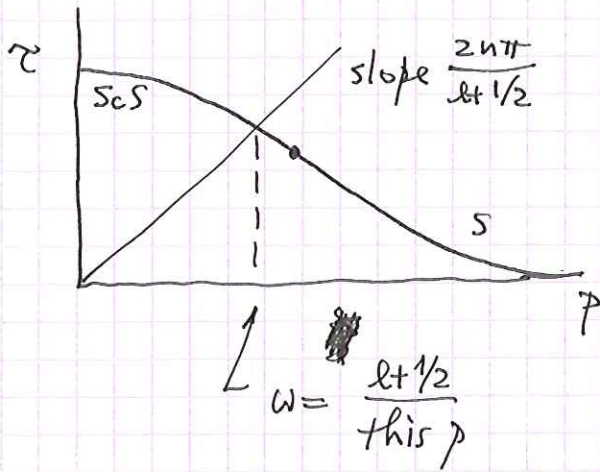
↑
caustic phase shift

$$\omega T(p) = 2\pi \left(n + \frac{1}{4} \right)$$

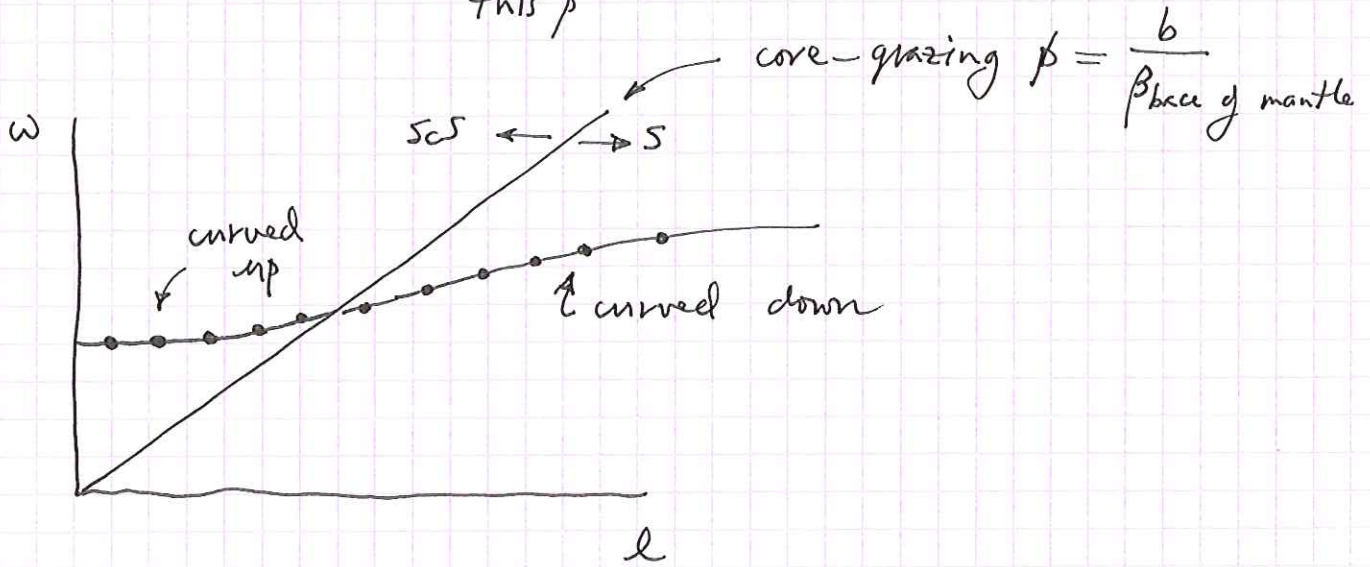
↑
mly diff

Schematically to find ω :

$$\tau(p) = \left(\frac{2n\pi}{l+1/2} \right) p$$



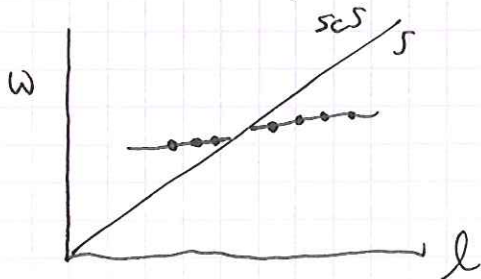
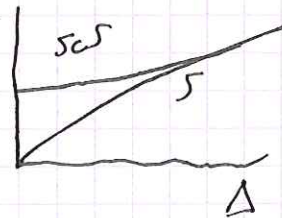
$$\text{or } = \left(\frac{2(n+1/4)\pi}{l+1/2} \right) p$$



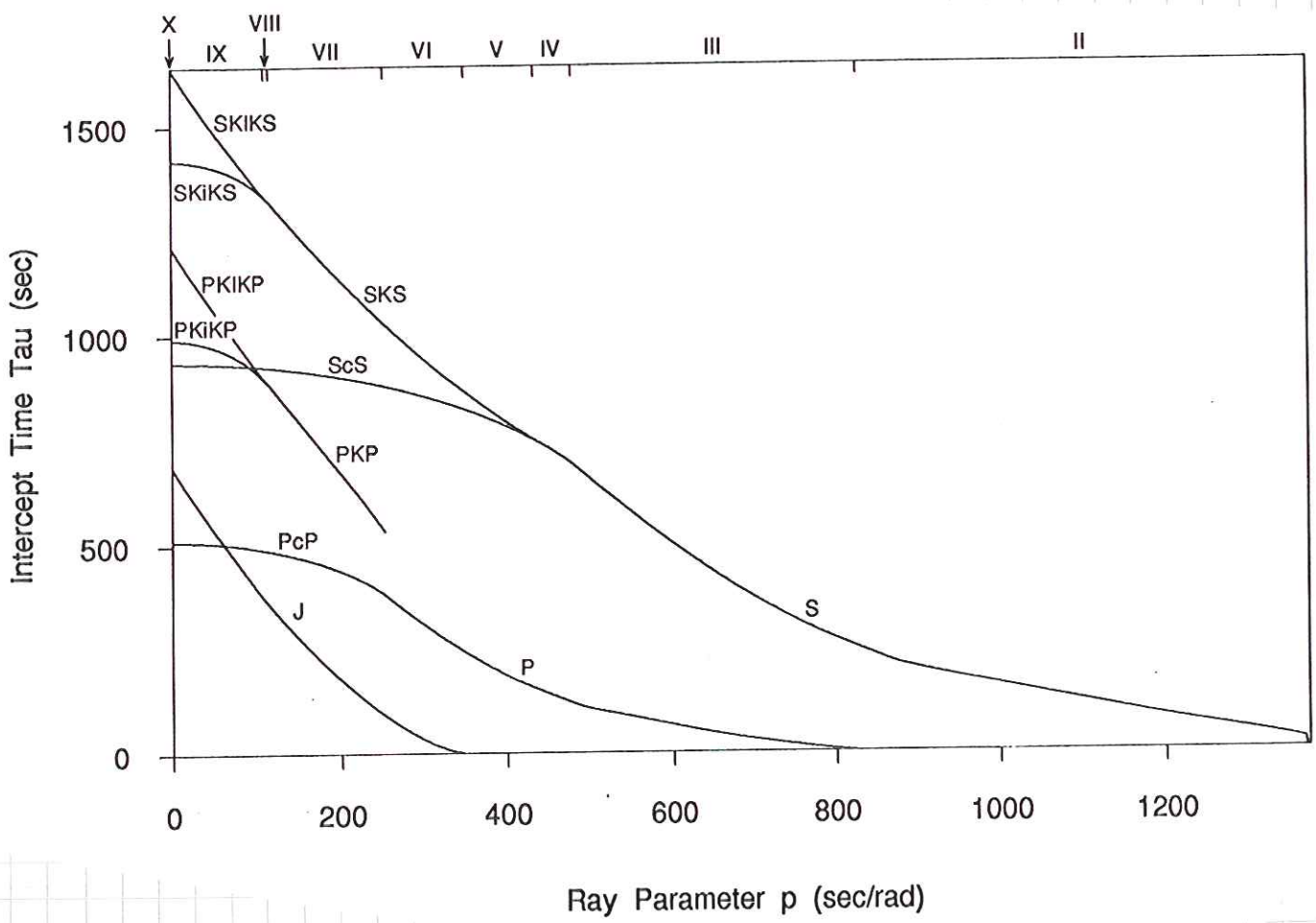
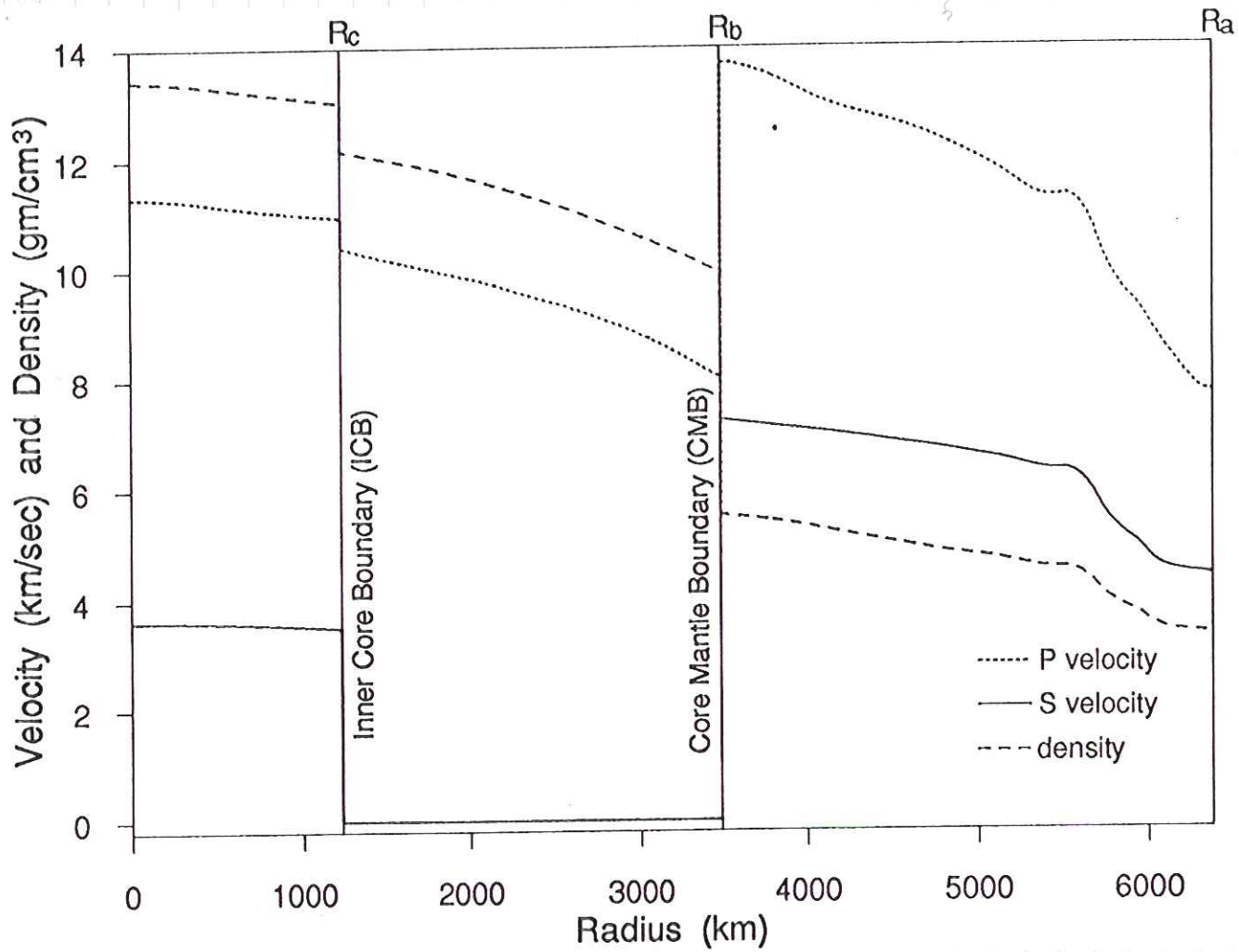
The inflection in the ω_l dispersion curves occurs at the core-grazing value of β . It's caused by the similar inflection of the $\tau(p)$ ~~curve~~ curve

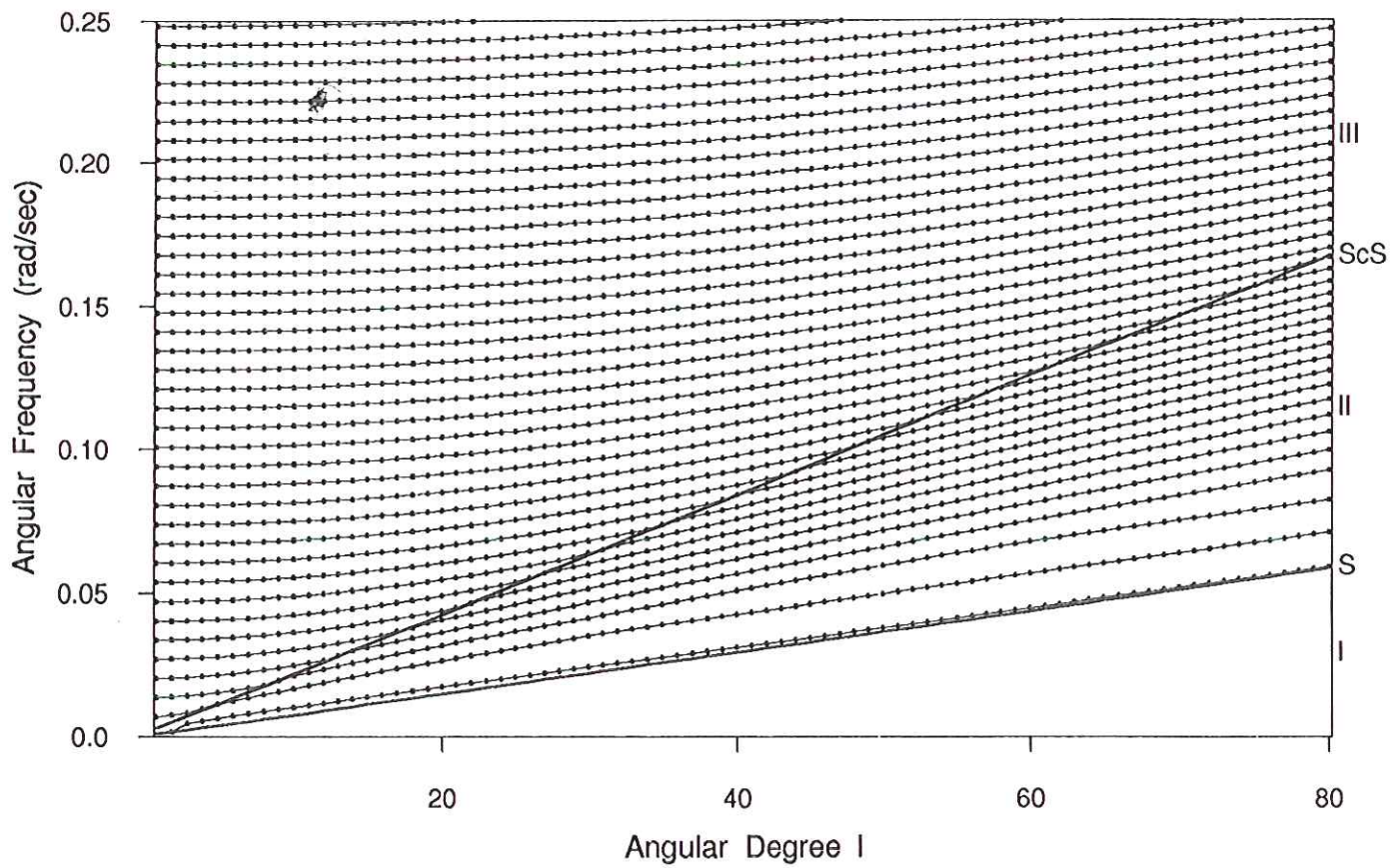
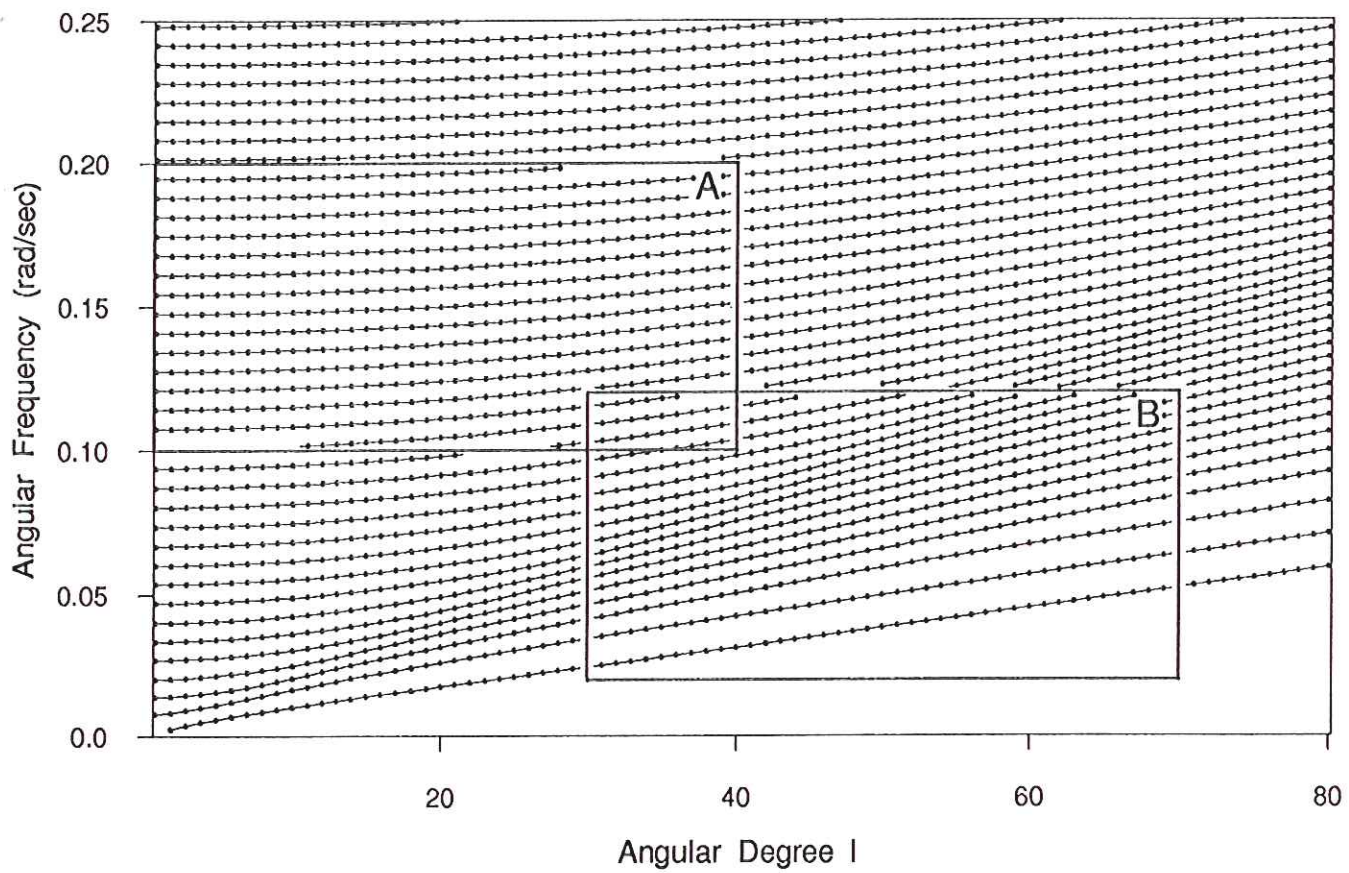
The caustic phase shift.

gives rise to a discontinuity in the dispersion curves.



This is in reality smoothed out by "quantum" tunneling effects that are not accounted for in my theory.





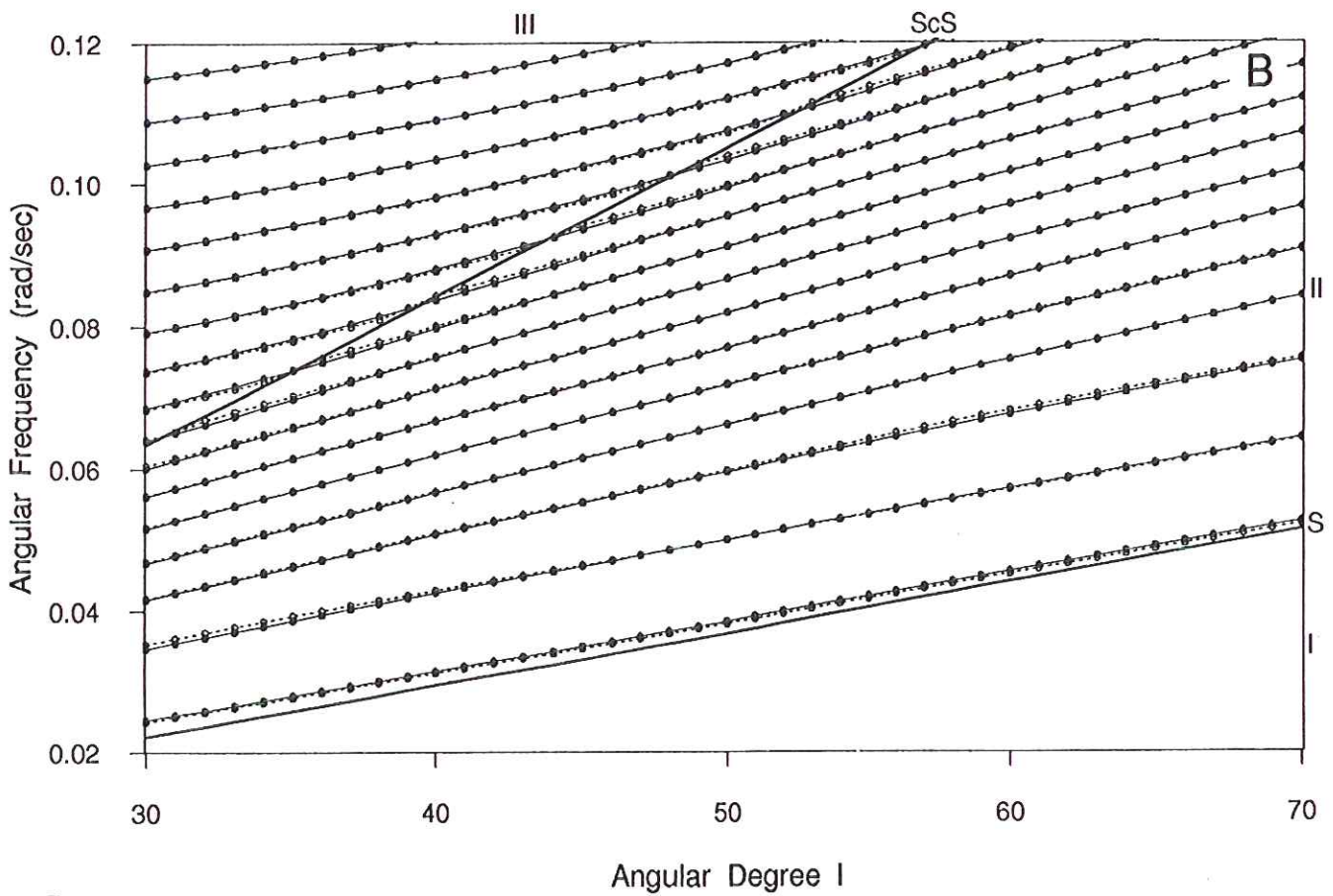
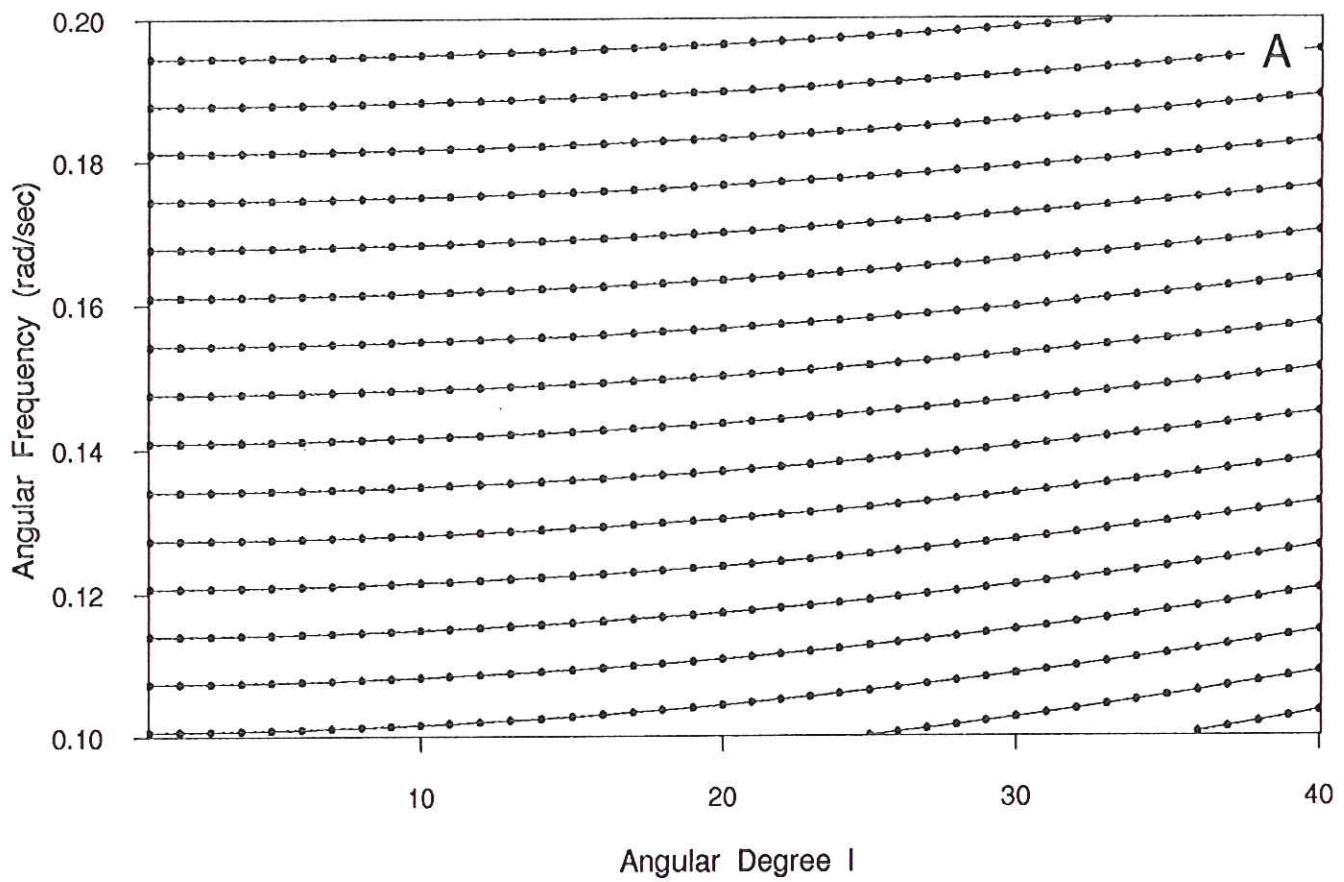


Fig. 17

Asymptotic toroidal eigenfunctions:

In the limit $\omega \rightarrow \infty$, $\beta = \frac{kt^{1/2}}{\omega}$ fixed the 2×2 toroidal system can be approximated by

$$\frac{d^2 z}{ds^2} + \omega^2 (1 - \beta^2 \beta^2 / r^2) z = 0$$

where $z = r (\rho\beta)^{1/2} W$, $s = \int_b^r \frac{dr}{\beta}$

The associated b.c. in this limit are

$$\frac{dz}{ds}(0) = \frac{dz}{ds} \left(\int_b^a \frac{dr}{\beta} \right) = 0.$$

JWKB ~~solutions~~ solutions are of the form:

$$z = (1 - \beta^2 \beta^2 / r^2)^{-1/4} \exp \left[\pm i \int_0^s \omega (1 - \beta^2 \beta^2 / r^2)^{1/2} ds \right]$$

For ScS equivalent modes:

$$W(r) \approx \frac{1}{r\sqrt{\rho\beta}} (1 - \beta^2 \beta^2 / r^2)^{-1/4} \cos \left[\omega \int_b^r \sqrt{\beta^{-2} - \beta^2 r^{-2}} dr \right]$$

or $\mu^{-1/2}$

$$W(r) = r^{-1} \left(\beta^{-2} - \beta^2 r^{-2} \right)^{-1/4} \cos \left[\omega \int_b^r \sqrt{\beta^{-2} - \beta^2 r^{-2}} dr \right]$$

↑ satisfies b.c. at CMB

Upper b.c. is satisfied if

$$\sin \left[\omega \int_b^a \sqrt{\beta^{-2} - \beta^2 r^{-2}} dr \right] = 0 \quad \text{or} \quad \sin \left(\frac{1}{2} \omega \tau_{ScS} \right) = 0$$

or $\omega \tau_{ScS} = 2n\pi$, as before.

Consider the normalization integral

$$\int_{\Phi} \rho s \cdot s \, dV = l(l+1) \int_a^b \rho W^2 r^2 \, dr$$

$$\int_a^b \rho W^2 r^2 \, dr = \frac{1}{2} \int_b^a \frac{dr}{\beta^2 \sqrt{\beta^{-2} - \beta^2 r^{-2}}} = \frac{1}{4} T$$

↑ from average of \cos^2
↑ the travel time

The properly normalized eigenfunction is thus

$$W(r) = \frac{2}{\omega_p^2 \sqrt{T_s} r \sqrt{\mu}} (\beta^{-2} - \beta^2 r^{-2})^{-1/4} \cos \left[\omega \int_b^a \sqrt{\beta^{-2} - \beta^2 r^{-2}} \, dr \right]$$

SCS-equivalent

or

$$W(r) = \frac{2}{\omega_p^2 \sqrt{T_s} r \sqrt{\mu}} (\beta^{-2} - \beta^2 r^{-2})^{-1/4} \cos \left[\int_b^a \omega \sqrt{\beta^{-2} - \beta^2 r^{-2}} \, dr - \frac{\pi}{4} \right]$$

↑ turning point

note: this is singular at turning point

this comes from solving the JWKB turning point connection problem

A uniformly valid result can be obtained using Airy functions near the turning point, or equivalently, the Langer approximation.

Toroidal Mode $2T_{10}$

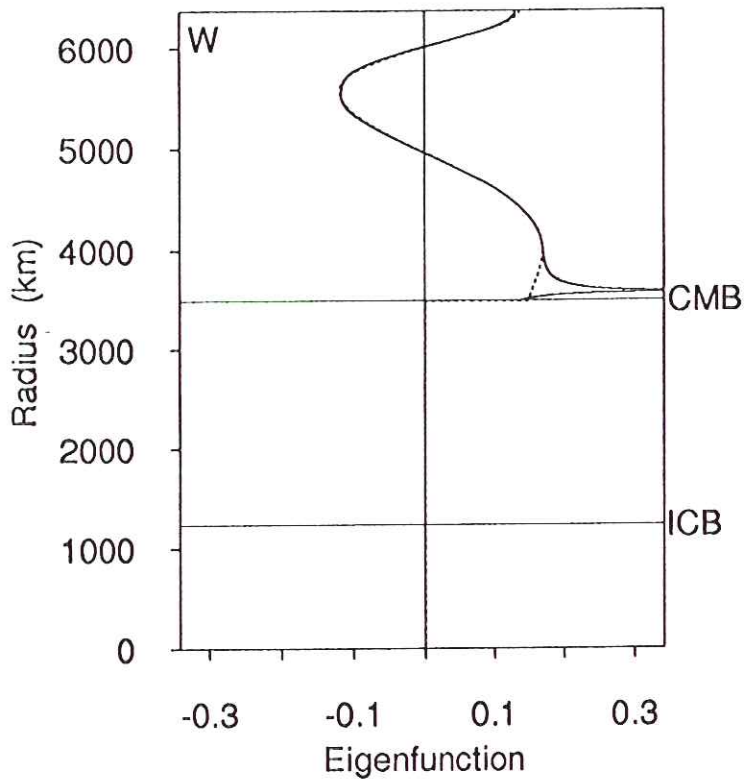


Fig. 16 (a)

Toroidal Mode $10T_{10}$

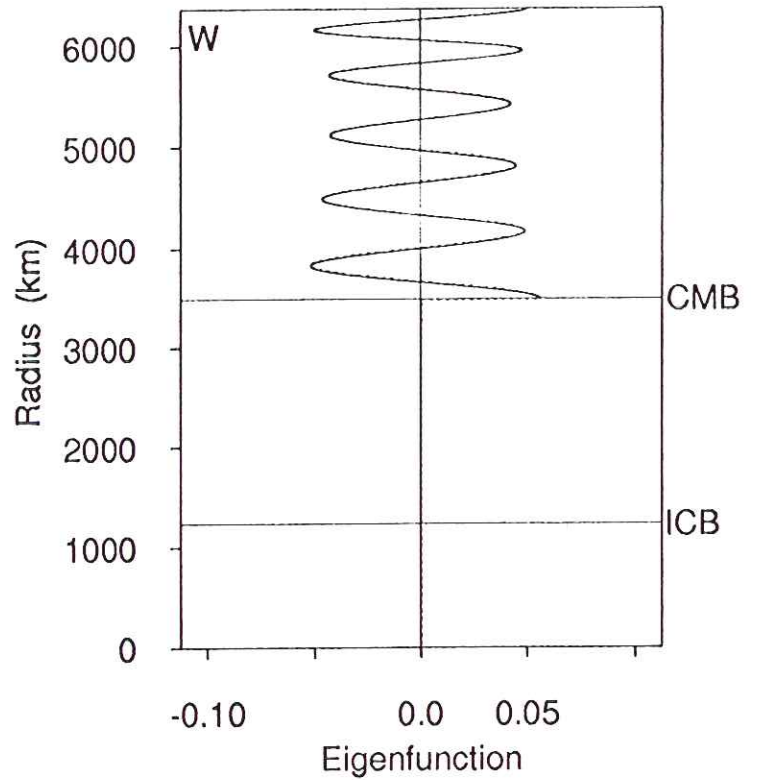


Fig. 16 (b)